Title
Characterizing the Role of PI3'-Kinase Signaling in BRAF-Mutated Melanoma

Author
Deuker, Marian Mitchell

Publication Date
2015

Peer reviewed|Thesis/dissertation

Characterizing the Role of PI3'-Kinase Signaling in BRAF-Mutated Melanoma

by

Marian M. Deuker

DISSERTATION

Submitted in partial satisfaction of the requirements for the degree of

DOCTOR OF PHILOSOPHY

in

Chemistry and Chemical Biology

in the

GRADUATE DIVISION

of the

UNIVERSITY OF CALIFORNIA, SAN FRANCISCO

Acknowledgments

Dr. Martin McMahon taught a week of my Chemical Biology course in January 2012. That fateful week served as my introduction to BRAF, and set into motion the course of events leading to the completion of this dissertation. As he spoke to the class, Martin's vim and vigor captivated my attention, and I decided to rotate in Martin's lab the following quarter. I would like to extend my deepest thanks to Martin for welcoming me into his lab, and for guiding me over these past three and a half years as I have matured as a scientist. Discussions with Martin never failed to reveal new ideas and invigorate my enthusiasm for my project. Words cannot fully express my gratitude towards Martin; I truly cannot imagine a better mentor to guide my graduate studies.

During my rotation, I benefited from the patient and intelligent mentorship of Dr. Victoria Marsh Durban. Vicky spent numerous hours teaching me mouse techniques and introducing me to the nuances of preclinical studies using genetically engineered mouse models. Beyond her scientific guidance, Vicky became a wonderful friend. My morning conversations with Vicky always brought happiness. After Vicky's departure, I turned to Dr. Jillian Silva for guidance. She became a wonderful mentor and friend, helping me immeasurably. As a graduate student in Martin's lab, I overlapped with two other graduate students, Joseph Juan and Shon Green. Our interactions helped me to think more critically about my project, and brought laughter to my mornings. I am so happy to have shared my hours in lab with Joe and Shon. I would like to thank all of the remaining members of the McMahon Lab for their support over the years: Dr. Allison Landman, Evan Markegard, Rachel O'Keefe, Dr. Paddy O'Leary, Dr. Daphne Pringle, Dr. Anny Shai, and Dr. Ed van Veen. My thesis committee contributed greatly to the

intellectual atmosphere of my UCSF experience. I offer my sincerest thanks to Dr. Rosemary Akhurst, Dr. Adil Daud, and Dr. Natalia Jura for their assistance.

I would like to thank my parents for introducing me to the world of books, and for supporting my decisions. Lastly, I would like to thank Aaron, for everything.

A portion of the material that appears in the introduction of this dissertation has been published previously, as indicated by the following citation. All material from the following review included in this dissertation was written by Marian M. Deuker.

Holderfield M*, **Deuker MM***, McCormick F, McMahon M. Targeting RAF kinases for cancer therapy: BRAF mutated melanoma and beyond. *Nat Rev Cancer* 2014; 14(7); 455-67.

***Co-first authorship**

This dissertation also includes material previously published in the following citation. Marian M. Deuker performed all experiments and wrote the text of the material from the following citation.

Deuker MM, Marsh Durban V, Phillips W, McMahon M. PI3'-Kinase Inhibition Forestalls the Onset of MEK1/2 Inhibitor Resistance in *BRAF*-Mutated Melanoma. *Cancer Discov* 2015; 5(2); 143-53.

Abstract

Phosphatidylinositide 3' (PI3')-lipid signaling cooperates with oncogenic $BRAF^{V600E}$ to promote melanomagenesis. Sustained PI3'-lipid production commonly occurs via silencing of the PI3'-lipid phosphatase PTEN or, less commonly, through mutational activation of *PIK3CA*, encoding the 110kDa catalytic subunit of PI3'-kinase-α (PI3Kα). To define the PI3K catalytic isoform dependency of *BRAF*-mutated melanoma, we utilized pharmacologic, isoform-selective PI3K inhibitors in conjunction with melanoma-derived cell lines and genetically engineered mouse (GEM) models. While $BRAF^{V600E}$/$PIK3CA^{H1047R}$ melanomas were sensitive to the anti-proliferative effects of selective PI3Ka blockade, inhibition of $BRAF^{V600E}$/$PTEN^{Null}$ melanoma proliferation required combined blockade of PI3Kα, δ and γ, and was insensitive to PI3Kβ blockade. In GEM models, isoform-selective PI3K inhibition elicited cytostatic effects, but significantly potentiated melanoma regression in response to $BRAF^{V600E}$ pathway-targeted inhibition. Interestingly, PI3K inhibition forestalled the onset of MEK inhibitor resistance in two independent GEM models of $BRAF^{V600E}$-driven melanoma. These results suggest that combination therapy with PI3K inhibitors may be a useful strategy to extend the duration of clinical response of *BRAF*-mutated melanoma patients to $BRAF^{V600E}$ pathway-targeted therapies.

Table of Contents

List of Tables

List of Figures

Background

Normal Skin Physiology and Melanoma Development

The skin plays an essential protective role, providing a barrier to shield the body from microbial, oxidative, mechanical, and chemical stresses. A complex milieu of cell types coexists within the epidermis to regulate these functions. The epidermis comprises primarily keratinocytes, which synthesize keratins and other structural proteins to maintain the cornification phenotype of the epidermis. Keratinocytes engage in perpetual movement, migrating from the basement membrane towards the surface of the epidermis as they divide and differentiate. In addition to keratinocytes, melanocytes also compose a small proportion of the basal cell population of the epidermis. Melanocytes are melanin-producing cells that extend dendritic processes among neighboring keratinocytes. Under physiological conditions, humans maintain a 1:5 ratio of melanocytes to basal keratinocytes (1). The melanin produced by melanocytes is packaged into melanosomes, which are then transferred along dendritic processes to keratinocytes. Typically one melanocyte extends dendrites to 36 associated keratinocytes. In the inner layers of the epidermis melanosomes form a protective shield over the nuclei of keratinocytes, whereas in the outer layers of the epidermis, melanosomes distribute more evenly. Merkel cells, which are associated with light touch sensation, are also found in the basal layer of the epidermis. Finally Langerhans cells, located primarily in the stratum spinosum layer of the epidermis, are antigen presenting immune cells that take up and process microbial antigens during skin infections.

During childhood, as the surface of the skin expands steadily, melanocytes proliferate constantly to maintain a stable ratio with the basal keratinocytes. Prior to cell division,

melanocytes retract their dendrites and detach from the basement membrane and keratinoctyes. After cell division, melanocytes recouple to the basement membrane and keratinocytes, to form another epidermal melanin unit. The half-life of adult melanocytes is poorly understood, but it is thought that proliferation continues at a low rate in response to specific stimulation such as wounding or ultraviolet (UV) light exposure. Melanoma arises from the unconstrained proliferation of melanocytes. Classically, the Clark model has described melanoma as a progressive disease comprising five histopathological steps: (1) common acquired melanocytic nevus; (2) melanocytic nevus with aberrant differentiation and melanocytic nuclear atypia; (3) radial growth phase of primary melanoma; (4) vertical growth phase of primary melanoma; (5) metastatic melanoma (2). However, this orderly categorization belies the clinical complexity of melanoma. About half of melanoma cases arise without clinically defined precursors, and while poorly understood, it is thought that melanoma can arise without melanocyte precursors passing through the "classical" progression steps. Further, the molecular mechanisms that regulate the transition from the radial growth phase (during which cell are thought to lack the capacity for metastasis) to the vertical growth phase (during which cells are fully capable of metastatic spread) remain enigmatic.

Mitogen Activated Protein Kinase (MAPK) Signaling

Hyperactivation of the mitogen activated protein kinase (MAPK) pathway has been identified as an early initiating event in melanomagenesis: although the majority of benign nevi display hyperactive MAPK pathway activity, the majority of nevi do not progress to melanoma, suggesting that MAPK pathway hyperactivation induces a brief burst of melanocyte proliferation followed by a period of senescent-like growth arrest that serves as a barrier to progression. The

loss of a tumor suppressor or the activation of an oncogene is necessary to cooperate with MAPK pathway hyperactivation to drive melanoma progression. Under physiological conditions, the MAPK pathway is activated when extracellular mitogens bind to a membrane receptor tyrosine kinase (RTK). Upon ligand binding, RTKs activate guanine exchange factors (GEFs), which in turn promote the removal of guanosine diphosphate (GDP) from Ras proteins. The high intracellular guanosine triphosphate (GTP) concentration allows Ras to rapidly bind a GTP molecule, and thus Ras assumes an active conformation. The MAPK signal cascade lies downstream of Ras: upon GTP binding Ras activates RAF kinases, which in turn phosphorylate MEK (mitogen activated protein kinase kinase) 1 and MEK2, which in turn phosphorylate ERK (extracellular signal-regulated kinase) 1 and ERK2. ERK1/2 activate numerous downstream targets to promote protein translation as well as cell proliferation, growth, and survival. Constitutive activation of the MAPK pathway in melanoma serves to decouple MAPK signaling from extracellular mitogenic signals. In 2004 sequencing efforts identified *BRAF* mutations in about half of all melanoma patients. This T1799A transversion in the 16th exon of *BRAF* leads to expression of a glutamic acid at position 600 of the BRAF protein, instead of the wild-type valine. The BRAF^{V600E} protein was shown to possess constitutive kinase activity, and by solving the crystal structure of the oncoprotein, it was demonstrated that a glutamic acid at position 600 of the activation loop mimics an activating phosphorylation event, thus inducing constitutive kinase activity.

Development of BRAF Targeted Inhibitors

In response to identification of the high frequency of BRAF^{V600E} expression in melanoma, pharmaceutical companies began to explore the therapeutic efficacy of targeting

$BRAF^{V600E}$ with small molecule kinase inhibitors. Plexxicon, a Bay Area-based pharmaceutical company, led the field with development of the PLX4032 (later named vemurafenib). Using a scaffold- and structure-based discovery approach, Plexxicon screened a library of 20,000 compounds against multiple structurally characterized kinases, with the goal of identifying protein kinase inhibitor scaffolds (3). This screen led to the identification of 238 compounds with activity against three kinases, and co-crystallographic analysis suggested that compounds with a monosubstituted 7-azaindole displayed increased affinity for participating in bonding interactions with the kinase hinge region. Development and screening of a library of analogs built around the 7-azaindole core demonstrated that a series of compounds containing a difluoro-phenylsulfonamide substructural motif achieved high potency for the $BRAF^{V600E}$ oncoprotein without simultaneous inhibition of many other kinases, including wild-type BRAF. Optimization of compounds containing the difluoro-phenylsulfonamide substructural motif led to the discovery of propane-1-sulfonic acid [3-(5-chloro-1H-pyrrolo[2,3-b]pyridine-3-carbonyl)-2,4-difluoro-phenyl]-amide (PLX4720), which inhibits $BRAF^{V600E}$ at a ten fold-lower concentration *in vitro* as compared to the concentration necessary to inhibit wild-type BRAF. Structural analysis revealed that PLX4720 achieves selectivity for the $BRAF^{V600E}$ oncoprotein because PLX4720 binds to the active, DFG-in, conformation of the kinase. Specifically, the sulfonamide moiety of PLX4720 is thought to interact differentially with the aspartic acid and phenylalanine of the DFG sequence when BRAF is in the active versus inactive conformation. Deprotonation of the nitrogen atom of the sulfonamide moiety favors interaction with the active kinase conformation, which is also favored by the V600E mutation. Cell culture experiments confirmed that PLX4720 preferentially inhibited the proliferation and ERK activation of human-derived cancer cell lines carrying the oncogenic *BRAF* allele as compared to cancer cell lines

carrying the wild-type *BRAF* allele. PLX4720 also displayed antitumor activity against a melanoma xenograft model in which athymic or SCID mice were implanted with melanoma cell lines expressing $BRAF^{V600E}$.

BRAF Inhibitors in Clinical Trials

Vemurafenib (also referred to as PLX4032, the clinical analogue of PLX4720) completed phase I/II clinical trials in 2010 (4). The initial groups of patients enrolled in this trial received a crystalline formulation of vemurafenib, which was subsequently found to possess poor bioavailability. Herculean medicinal chemistry efforts resulted in reformulation of vemurafenib as a highly bioavailable microprecipitated-bulk-powder. After identification of the recommended phase II dose, the trial enrolled an extension cohort of advanced melanoma patients whose disease carried the $BRAF^{V600E}$ mutation. Among the 32 *BRAF*-mutated patients composing the extension cohort, 26 of the 32 (81%) patients demonstrated a response, as assessed by the Response Evaluation Criteria in Solid Tumors (RECIST), version 1.0. Two of these patients had a complete response (CR), and the other 24 had a partial response (PR). These promising results motivated the initiation of a multicenter phase II trial designed to test the overall response rate of *BRAF*-mutated melanoma patients receiving vemurafenib treatment; of the 132 patients enrolled in the study, the independent review committee reported an overall response rate of 53%, with a CR rate of 6% (5). Results from the pivotal phase III randomized clinical trial (published before the aforementioned phase II trial), in which patients with advanced $BRAF^{V600E}$-mutated melanoma received either vemurafenib or dacarbazine therapy, indicated that at 6 months, overall survival was 84% in the vemurafenib group and 64% in the

dacarbazine group (6). Of the 549 patients eligible for PFS analysis, the median PFS in the vemurafenib group was 5.3 months compared to 1.6 months in the dacarbazine group. Finally, among the 439 patients eligible for tumor response analysis (RECIST, version 1.1), 48% of patients in the vemurafenib group had a confirmed objective response and 5% of patients in the dacarbazine group had a confirmed objective response. Based on these promising clinical trial results, vemurafenib achieved FDA approval for the treatment of advanced, $BRAF^{V600E}$-mutated melanoma patients on August 17th, 2011. Shortly thereafter, the FDA granted approval to a second BRAF inhibitor, dabrafenib, for the treatment of advanced $BRAF^{V600E/K}$-mutated melanoma patients.

Mechanisms of Resistance to BRAF Inhibitors

The approval of BRAF-targeted inhibitors for the treatment of advanced *BRAF*-mutated melanoma patients changed the paradigm of treatment for this subset of melanoma patients, and offered a glimmer of hope to patients who had historically faced an utterly bleak prognosis. However, despite the high rate of response to BRAF inhibitors, the median length of progression free survival for patients receiving BRAF inhibitor therapy remains limited to less than six months, thus dramatically limiting the clinical utility of BRAF inhibitors. Upon observing the high frequency at which patients developed resistance to single agent BRAF inhibitors, intensive efforts were undertaken to characterize mechanisms of resistance, and to develop additional targeted therapies to attenuate the activity of these resistance pathways. Initial attempts to anticipate resistance mechanisms were informed by experience with acquired resistance to imatinib in BCR-ABL mutated leukemia, where mutation of the "gatekeeper" threonine prevents

drug binding without drastically affecting normal kinase activity (7, 8). Surprisingly, although engineering of mutations at the analogous gatekeeper residue (T529) in BRAF confers vemurafenib resistance *in vitro*, T529 mutations have never been reported in BRAF inhibitor resistant patient tumor samples (8). One possible explanation for the failure to find such an obvious, and highly predicted, mechanism of resistance may be that cells expressing BRAF doubly mutated at codons 529 and 600 are not viable in the absence of drug. Therefore, there would be no reservoir of such cells prior to drug treatment and this would consequently not score as a mechanism of drug resistance. Although Marais and colleagues have shown that a myeloid cell line remains viable in the absence of BRAF inhibitor when transfected with BRAF doubly mutated at codons 529 and 600 (8), this observation is likely cell-type specific and may also reflect the outgrowth of cells transduced with lower—and thus non-toxic—levels of doubly mutated BRAF.

Despite the absence of T529 mutations in BRAF, numerous other mechanisms of acquired resistance to BRAF inhibitors that contribute to clinical drug resistance have been described. The majority of resistance mechanisms promote re-activation of the MAPK signaling pathway in the presence of BRAF inhibitor (Figure 4). For example, mutational activation of *NRAS*, *MEK1* or *MEK2* can reactivate the MAP kinase pathway in the presence of BRAF inhibition (9-12) and elevated CRAF protein levels have also been shown to confer resistance to BRAF inhibition in cell culture melanoma models (12, 13). CRAF protein elevation has yet to be identified in clinical samples of BRAF inhibitor resistance, and it has been shown that in some contexts CRAF negatively regulates BRAF-V600E (14), so further analysis is necessary to determine the clinical relevance of CRAF protein elevation as a bona fide BRAF inhibitor resistance mechanism. Through an unbiased screen, the serine/threonine MAP kinase kinase

kinase (MAP3K) COT kinase (encoded by *MAP3K8*) was shown to activate MEK in the presence of BRAF inhibition (15). Importantly, elevated *COT* copy number and mRNA expression was identified in biopsy specimens of metastatic melanoma following vemurafenib treatment. Overexpression of the mutant BRAF protein itself has also been reported, further emphasizing the importance of increased expression of the drug target as a relevant mechanism of cancer drug resistance (16, 17). Additionally, the identification of BRAF-V600E splice-variants, which endow the proteins with the ability to dimerize in a RAS-independent manner and increases the kinase activity of the proteins, represents the only resistance mechanism that involves a structural change to BRAF itself and one of the first examples where altered mRNA splicing can render an oncoprotein resistant to a drug (18).

Vertical MAPK Pathway Inhibition: BRAFi + MEKi

The high frequency of mutations that confer BRAF inhibitor resistance through reactivation of MAPK signaling despite the presence of BRAF inhibition suggested that inhibition of MEK1/2, the direct downstream target of BRAF, might provide clinical benefit after progression on BRAF inhibitor monotherapy. Unfortunately, clinical data suggest limited efficacy of MEK inhibitor monotherapy for *BRAF*-mutated melanoma patients with BRAF inhibitor resistant disease. Within a cohort of 40 patients who had progressed on either vemurafenib or dabrafenib monotherapy, subsequent treatment with the MEK1/2 inhibitor trametinib offered only a 1.8 month median PFS and a 5.8 month median OS (19). Only two patients within the cohort had a complete or partial response and both of these patients had discontinued BRAF inhibitor therapy due to adverse events rather than the onset of drug-resistant

disease. Thus the clinical efficacy of second-line MEK inhibitor monotherapy to treat BRAF inhibitor resistant disease seems limited. Another strategy to forestall the onset of BRAF inhibitor resistance developed based on the idea that concurrent inhibition of BRAF plus MEK1/2 would more potently suppress MAPK pathway activity, and thus extend the duration of response to BRAF inhibition. In a phase III clinical trial testing this hypothesis in a cohort of 423 advanced $BRAF^{V600E/K}$-mutated melanoma patients, the median PFS was 9.3 months in the dabrafenib plus trametinib cohort and 8.8 months in the dabrafenib cohort (20). The overall response rate was 67% in the dabrafenib plus trametinib cohort and 51% in the dabrafenib cohort. A second phase III clinical trial was performed evaluating vemurafenib plus cobimetinib (also referred to as GDC-0973, a MEK1/2 inhibitor developed by Genentech) treatment to vemurafenib monotherapy. In this trial the median PFS was 9.9 months in the vemurafenib plus cobimetinib cohort and 6.2 months in the vemurafenib cohort (21). Together results from these clinical trials suggest that while concurrent BRAF plus MEK inhibitor therapy is superior to BRAF inhibitor monotherapy, the extension of PFS is relatively modest, and median PFS remains under twelve months. Notably, concurrent treatment with MEK1/2 inhibitors reduces BRAF inhibitor-associated toxicities that arise from the ability of BRAF inhibitors to paradoxically activate MAPK signaling in cells harboring wild-type BRAF or mutationally activated RAS. Therefore, BRAF plus MEK inhibitor therapy has been adapted as a standard of care for advanced, *BRAF*-mutated melanoma patients. However, the rapid development of resistance to this combination drug regimen highlights the importance of identifying MAPK pathway-independent targets that can be inhibited therapeutically to extend the duration of response to MAPK pathway-targeted therapies.

Phosphatidylinositol 3'-Kinase (PI3K) Signaling

The phosphatidylinositol 3'-kinase (PI3K) signaling pathway has emerged as a prime candidate for several reasons. Approximately 50% of *BRAF*-mutated melanoma patients display concurrent dysregulation of the PI3K pathway. The most common PI3K pathway mutation observed in *BRAF*-mutated melanoma involves loss of the PTEN tumor suppressor, but other PI3K pathway components including *PIK3CA, PIK3CG, RAC1, AKT3, TSC1,* and *MTOR* are also mutated in a subset of patients. Under physiological conditions, the PI3K pathway is activated following RTK stimulation, which recruits the PI3K heterodimer, comprising the regulatory p85 subunit and the catalytic p110 subunit, to translocate to SH2 domains associated with activated RTKs. Upon heterodimerization at the plasma membrane, the catalytic p110 subunit of PI3K phosphorylates phosphatidylinositol 4,5-bisphosphate (PIP_2) at the 3' position, to generate phosphatidylinositol 3,4,5-triphosphate (PIP_3). PIP_3 acts as a secondary messenger to recruit a subset of pleckstrin homology (PH) domain containing proteins to the plasma membrane. The best-characterized effector of PIP_3 is AKT (also referred to as protein kinase B or PKB). Upon binding to PIP_3 at the plasma membrane, AKT is phosphorylated by mammalian target of rapamycin complex 2 (mTORC2) at serine 473 and by phosphatidylinositol 4,5-bisphosphate (PDK1) at threonine 308. These two phosphorylation events allow for full activation of AKT, promoting activities such as protein translation, cellular growth, cellular proliferation, suppression of apoptosis, and glycogen synthesis. The PI3K pathway is mutated in numerous solid tumors and hematological malignancies beyond melanoma, and has thus been an area of intensive drug discovery efforts for some time. Further, the ability of p110 catalytic

isoform overexpression to transform chicken embryonic fibroblasts in cell culture emphasizes the oncogenic potential of PI3K signaling.

In addition to the importance of PI3K signaling in melanomagenesis, it has been suggested that PI3K signaling plays a frequent role in the development of BRAF inhibitor resistance. Approximately 30% of patients develop MAPK pathway-independent mechanisms of resistance (22). Initial reports suggest that the majority of MAPK pathway-independent mechanisms of resistance involve alterations that lead to upregulation of the PTEN-PI3K-AKT signaling axis. Moreover, elevated expression of either platelet-derived growth factor receptor-β (PDGFRβ) or insulin-like growth factor I receptor (IGF1R) expression was identified in cultured cells and in specimens from patients with vemurafenib-resistant melanomas. It is claimed that PDGFRβ or IGF1R signaling allows for activation of MAP kinase pathway-independent pro-survival signaling pathways, such as the PI3'-K/AKT axis, which render cells resistant to the effects of BRAF inhibition (9, 23).

PI3K Inhibitors

Despite ample evidence corroborating the oncogenicity of PI3K signaling, pan class I PI3K inhibitors, which target all four of the class I catalytic p110 isoforms (p110α, p110β, p110δ, and p110γ) have performed poorly to date in clinical trials. The lack of efficacy for these compounds may derive from the fact that because PI3K signaling is critical for many important physiological processes, such as insulin signaling, the therapeutic window may be too narrow to potently suppress intratumoral pan class I PI3K signaling without toxicity in other tissues. Therefore, recent years have witnessed renewed efforts by pharmaceutical companies to develop

isoform specific class I PI3K inhibitors. It is hypothesized that the therapeutic window of class I PI3K inhibition may be broadened if only the isoform(s) relevant to tumor pathology is inhibited, without unnecessary inhibition of the isoforms critical for normal processes. The success of isoform selective PI3K inhibitors remains to be tested clinically.

Genetically Engineered Mouse (GEM) Models of Melanoma

After the high frequency of $BRAF^{V600E}$ oncoprotein expression in human melanoma was discovered, the McMahon Laboratory set out to model this genetic subtype of melanoma in mice. To that end, a genetically engineered mouse (GEM) was created carrying an allele that expresses wild type *BRaf* from the endogenous locus prior to exposure to Cre recombinase, but expresses the $BRaf^{VE}$ oncogene from the endogenous locus after Cre-mediated recombination of the genetically engineered allele (24). This allele, named the $BRaf^{CA}$ (Cre-activatable) allele, was generated through homologous recombination of embryonic stem cells to insert a vector into the normal *BRaf* allele after exon 14. The targeting vector contains a region of homology to exon 14 followed by a loxP-flanked cassette engineered to contain the 3'-382bp of intron 14, human *BRAF* cDNA encoded by exons 15-18, and the natural *BRaf* polyadenylation sequences followed by a positive selection marker derived from pBig. The positive selection cassette consists of the PGK promoter, a neomycin resistance gene and is followed by a downstream selectable cassette with a triple transcriptional stop and polyadenylation sequence from SV40 to prevent transcriptional read through to the loxP site. The second loxP site is followed by mouse cDNA encoding the mutated exon 15 followed by a sequence homologous to the region of the endogenous locus between exons 15 and 16, and finally a herpes simplex virus thymidine kinase

type 1 gene (HSV-TK) to act as a conditional negative-selection marker gene. By combining the *BRaf*^{CA} allele with the *Tyr::CreER* transgene, which encodes conditionally active CreER^{T2} under the control of the tyrosinase promoter which is active specifically in melanocytes, mice express the BRAF^{V600E} oncoprotein in a conditional manner only after melanocytes are exposed to 4-hydroxytamoxifen (25). As the genetics of human melanomagenesis predict, expression of BRAF^{V600E} in mouse melanocytes is insufficient to induce melanoma (26). Rather, activation of BRAF^{V600E} in mouse melanocytes induces highly pigmented lesions that do not progress to melanoma, and instead recapitulate the benign nevi that form in humans upon BRAF^{V600E} expression in epidermal melanocytes. However, by combining mice carrying homozygous floxed alleles of *Pten* (*Pten*$^{lox/lox}$) with the *Tyr::CreER BRaf*^{CA} mice, such that topical 4-hydroxytamoxifen application simultaneously activates BRAF^{V600E} expression and silences PTEN expression in melanocytes, mice develop melanoma with 100% penetrance that faithfully recapitulates the human disease.

More recently, the McMahon Laboratory developed a second GEM model of melanoma also built upon PI3K pathway activation in cooperation with oncogenic *BRAF*. In this second melanoma model, the *Tyr::CreER BRaf*^{CA} mice were combined with mice carrying a modified *Pik3ca*^{lat} allele (*Pik3ca*$^{lat\text{-}1047R}$) in which expression of normal p110α is converted to mutationally activated p110α^{H1047R} by Cre recombinase activity. Melanocyte specific expression of BRAF^{V600E} cooperated with mutationally activated p110α^{H1047R} to elicit melanoma.

Introduction

Over the past fifteen years, key genetic lesions that initiate melanomagenesis, promote disease progression and remain necessary for melanoma maintenance have been identified (27, 28). Approximately 50% of melanomas express mutationally activated $BRAF^{V600E}$, leading to constitutive activation of the $BRAF^{V600E}$→MEK1/2→ERK1/2 mitogen-activated protein (MAP) kinase pathway (29). The importance of this pathway in melanoma maintenance is highlighted by the ability of $BRAF^{V600E}$ pathway-targeted inhibitors to elicit dramatic tumor regression in *BRAF*-mutated, advanced melanoma patients (30-32). Although the response rate of such patients is high, the depth and durability of response is limited by the onset of drug resistant disease that is largely refractory to additional $BRAF^{V600E}$ pathway-targeted therapy (33, 34). Therefore, it is critical to identify signaling pathways that contribute to *de novo* or acquired drug resistance, and to determine if pharmacological blockade of these pathways can increase the response rate or the durability of response to $BRAF^{V600E}$ pathway-targeted therapies. Although multiple mechanisms of acquired drug resistance have been documented, it remains unclear the extent to which parallel inhibition of signaling pathways will enhance melanoma patient responses (9, 22).

Using genetically engineered mouse (GEM) models, we previously demonstrated that either PTEN silencing or mutationally activated $PIK3CA^{H1047R}$ cooperates with $BRAF^{V600E}$ to elicit metastatic melanoma. However, $BRAF^{V600E}$/$PIK3CA^{H1047R}$ melanomas grew more slowly than similarly elicited $BRAF^{V600E}$/$PTEN^{Null}$ melanomas (35). In addition, although a pan-class I PI3K inhibitor (BKM120) significantly potentiated the ability of a $BRAF^{V600E}$ inhibitor (LGX818) to induce regression of autochthonous $BRAF^{V600E}$/$PTEN^{Null}$ melanomas, BKM120 was largely ineffective as a single agent (35). Given the frequency of alterations in PI3'-lipid

signaling in *BRAF*-mutated melanoma (26, 36-38), we wished to explore the role of PI3K signaling in melanoma progression and maintenance, as well as the therapeutic implications of targeting this pathway using isoform-selective inhibitors. Our studies reveal that the difference in growth rate between $BRAF^{V600E}$/$PIK3CA^{H1047R}$ and $BRAF^{V600E}$/$PTEN^{Null}$ melanomas is likely due to the strength of PI3K pathway activation. However, potent blockade of PI3K signaling in either $BRAF^{V600E}$/$PIK3CA^{H1047R}$ or $BRAF^{V600E}$/$PTEN^{Null}$ melanomas elicited largely cytostatic effects. Finally, and most interestingly, combined blockade of $BRAF^{V600E}$ and PI3K signaling significantly enhanced the depth and durability of the response of $BRAF^{V600E}$/$PIK3CA^{H1047R}$ or $BRAF^{V600E}$/$PTEN^{Null}$ melanoma to the MEK1/2 inhibitor GDC-0973. These data provide a scientific rationale for the clinical deployment of such regimens for *BRAF*-mutated melanoma patients in which the PI3K pathway is activated either by *PTEN* silencing or *PIK3CA* mutation.

Results

PTEN is reported to have both phosphatase-dependent and -independent tumor suppressor activities (39-41). To address whether differences in growth rate between $BRAF^{V600E}$/$PIK3CA^{H1047R}$ and $BRAF^{V600E}$/$PTEN^{Null}$ melanoma reflect a role for phosphatase-independent tumor suppressor activities of PTEN, we compared the growth rate of *BRAF*-mutated melanomas in *Tyr::CreER; BRaf*^{CA} mice that were homozygous for the *Pten*$^{lox4-5}$ allele or either heterozygous or homozygous for the conditional Cre-activated *Pik3ca*$^{lat-1047R}$ (*Pik3ca*^{lat} hereafter) allele (Fig. 1A). As shown previously (35), $BRAF^{V600E}$/$PTEN^{Null}$ melanomas grew more rapidly than $BRAF^{V600E}$/$PIK3CA^{H1047R}$ melanomas arising in heterozygous *Pik3ca*$^{lat/+}$ mice (Fig. 1A). However, $BRAF^{V600E}$/$PIK3CA^{H1047R}$ melanomas arising in homozygous *Pik3ca*$^{lat/lat}$ mice grew significantly more rapidly than $BRAF^{V600E}$/$PTEN^{Null}$ melanomas, suggesting that differences in melanoma growth rate between $BRAF^{V600E}$/$PIK3CA^{H1047R}$ and $BRAF^{V600E}$/$PTEN^{Null}$ melanoma are likely due to the magnitude of PI3K pathway activation. In addition, cell lines derived from $BRAF^{V600E}$/$PTEN^{Null}$/$CDKN2A^{Null}$ (B10C) or $BRAF^{V600E}$/$PIK3CA^{H1047R/H1047R}$/$CDKN2A^{Null}$ (BP_2C) melanomas grew more rapidly *in vitro* than did a cell line derived from a $BRAF^{V600E}$/$PIK3CA^{H1047R/+}$/$CDKN2A^{Null}$ (BPC) melanoma (unpublished observation).

To determine the PI3K isoform dependence of *BRAF*-mutated melanoma, we treated BPC and B10C melanoma cell lines with pharmacological inhibitors of PI3K (Supp. Table 1). BPC melanoma cells treated with BYL719, a selective inhibitor of PI3'-kinase-α (PI3Kα) (42), displayed a robust reduction in cell proliferation over a 72-hour time period and colony forming ability over a ten-day period (Figs. 1B & 1C). By contrast, BYL719 treatment of B10C melanoma cells elicited only a modest reduction in short-term cell proliferation and had no effect

on long-term colony formation (Figs. 1B & 1C). Indeed, there was a greater than 10-fold difference between the concentration of BYL719 required for 50% inhibition of proliferation (GI_{50}) of BPC versus B10C cells (Fig. 1D). In addition, the BP_2C melanoma cell line derived from homozygous *Pik3ca*$^{lat/lat}$ mice displayed similar sensitivity to BYL719 as did the BPC cells (Figs. S1A & S1B). Thus, $BRAF^{V600E}$/$PIK3CA^{H1047R}$ melanoma cells display the predicted genotype-drug response phenotype relationship. By contrast, $BRAF^{V600E}$/$PTEN^{Null}$ melanoma cells appear not to depend solely on PI3Kα for their proliferation.

To examine the effects of PI3Kα blockade on signal pathway activity, extracts of BPC or B10C melanoma cells treated with BYL719 (5μM) were subjected to immunoblot analysis (Fig. 1E). In BPC cells, BYL719 elicited a complete and sustained inhibition of pAKT (pS473) over 72 hours. We also noted diminished phosphorylation of downstream pathway components of PI3K→AKT signaling including PRAS40 and 4E-BP1 (Fig. 1E). By contrast, BYL719-treated B10C cells displayed only a partial and transient inhibition of pAKT with almost no effect on pPRAS40 or p4E-BP1.

Since $BRAF^{V600E}$ and PI3K signal cooperatively through mTORC to regulate melanoma cell proliferation (43), we investigated whether PI3Kα inhibition would enhance the effects of $BRAF^{V600E}$ inhibition in BPC or B10C melanoma cells. While single agent $BRAF^{V600E}$ (LGX818) (44) or PI3Kα (BYL719) inhibition potently suppressed BPC melanoma cell proliferation, combined treatment elicited a significantly greater inhibition of cell proliferation at 24, 48, and 72 hours (Fig. 1F). Further, while inhibition of PI3Kα suppressed pPRAS40, pRPS6 and p4EB-P1 in BPC melanoma cells, combined inhibition of both $BRAF^{V600E}$ and $PIK3CA^{H1047R}$ signaling elicited a more robust inhibition of these phosphorylation events (Fig. 1G). Similar observations were made in the independently derived BP_2C melanoma cell line

(Fig. S1C). By contrast, while $BRAF^{V600E}$ inhibition (LGX818) potently suppressed B10C cell proliferation, addition of BYL719 did not significantly enhance the anti-proliferative effects of $BRAF^{V600E}$ inhibition at any time point (Fig. 1F). In B10C cells, LGX818 inhibited pERK but had little effect on pRPS6 or p4E-BP1 (Fig. 1G). Although treatment of B10C cells with BYL719 elicited a modest decrease in pAKT there was no effect on pPRAS40, pRPS6 or p4E-BP1. Most importantly, combined treatment of B10C cells with LGX818 plus BYL719 displayed no cooperative effects on pPRAS40, pRPS6 or p4E-BP1. Together, these data demonstrate that inhibition of PI3Kα enhanced the effects of $BRAF^{V600E}$ inhibition in $BRAF^{V600E}$/$PIK3CA^{H1047R}$ but not in $BRAF^{V600E}$/$PTEN^{Null}$ melanoma cells.

The anti-proliferative activity of PI3Kα selective inhibition on $BRAF^{V600E}$/$PIK3CA^{H1047R}$ cells *in vitro* prompted us to design a preclinical trial in mice to test the ability of BYL719, either alone or in combination with LGX818, to elicit regression of autochthonous $BRAF^{V600E}$/$PIK3CA^{H1047R}$ melanomas. To that end, $BRAF^{V600E}$/$PIK3CA^{H1047R}$ melanomas were initiated on the back skin of adult *Tyr::CreER; $BRaf^{CA}$; $Pik3ca^{lat/+}$* mice. In this scenario, melanomas are elicited by the cooperative action of two dominantly acting oncogenes: $BRAF^{V600E}$ and $PIK3CA^{H1047R}$ (35, 45). Seven weeks post-initiation (p.i), mice were randomized to receive vehicle, LGX818, BYL719, or combined LGX818 plus BYL719 treatment, with melanoma size measured weekly. Pharmacodynamic analysis of pAKT inhibition in $BRAF^{V600E}$/$PIK3CA^{H1047R}$ melanomas indicated the need to dose BYL719 twice daily to achieve maximal target inhibition (Fig. S1D).

Single agent BYL719 initially elicited modest melanoma regression (<30%), followed by a prolonged cytostatic effect (Fig. 1H). By contrast, single agent LGX818 elicited profound melanoma regression. Importantly, the combination of BYL719 plus LGX818 promoted

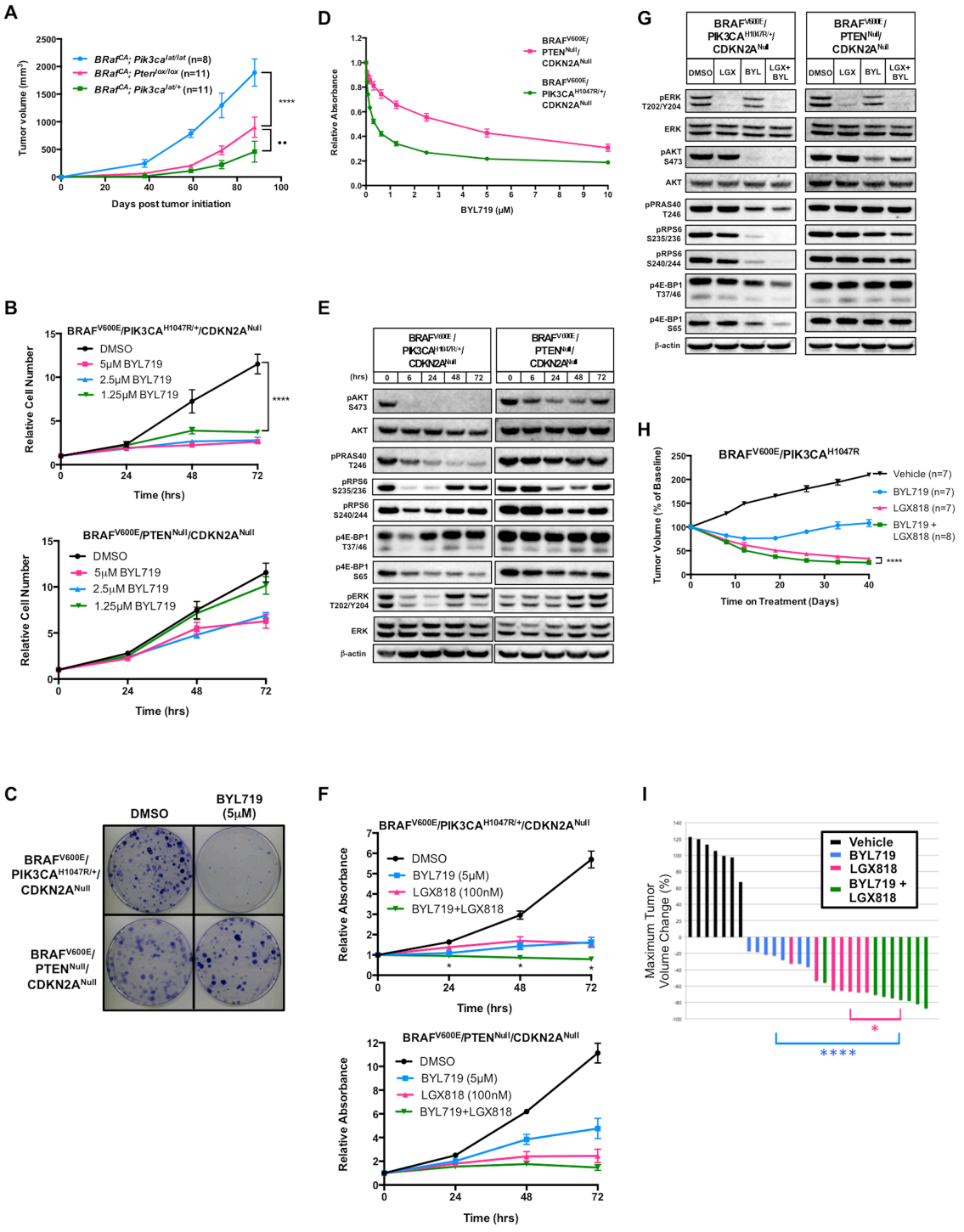

Figure 1: Autochthonous BRAF^{V600E}/PIK3CA^{H1047R} melanomas and cell lines are sensitive to PI3Kα-selective inhibition

(A) Melanoma was initiated in *Tyr::CreER; BRaf^{CA}* mice carrying *Pten$^{lox/lox}$* or either heterozygous or homozygous for *Pik3ca^{lat}* by topical application of 4-hydroxytamoxifen (4-HT), with melanoma growth assessed for 88 days. Average tumor volumes (mm^3 ± SEM) were measured starting at day 38 days p.i. Asterisks indicate significant difference in melanoma

Figure 1 cont.: Autochthonous BRAF^{V600E}/PIK3CA^{H1047R} melanomas and cell lines are sensitive to PI3Kα-selective inhibition

(A cont.) growth between *Tyr::CreER; BRaf^{CA}; Pik3ca$^{lat/lat}$* and *Tyr::CreER; BRaf^{CA}; Pten$^{lox/lox}$* mice and filled circles indicate significant difference between *Tyr::CreER; BRaf^{CA}; Pik3ca$^{lat/+}$* and *Tyr::CreER; BRaf^{CA}; Pten$^{lox/lox}$* mice (2-way ANOVA, ••, *p<0.005, ****, p<0.0001*).
(B) BPC or B10C melanoma cells were cultured in the presence of the indicated concentrations of BYL719 with cells counted every 24 hours for 72 hours. Cell counts are indicated as change in cell number relative to the number of cells at the initiation of drug treatment with error bars representing standard error of the mean (SEM). Asterisks indicate significant difference between DMSO and 1.25μM BYL719 (2-way ANOVA, *p<0.0001*).
(C) BPC or B10C melanoma cells were cultured in the presence of BYL719 (5μM) for a period of nine days before being fixed and stained with Crystal Violet.
(D) BPC or B10C melanoma cells were cultured in the presence of the indicated concentrations of BYL719 for 72 hours before being fixed and stained with Crystal Violet. Crystal Violet staining was quantified by solubilizing the fixed dye and assessing the absorbance at 562nm. Values are normalized to DMSO control and error bars represent SEM.
(E) Lysates of BPC or B10C melanoma cells, treated for the indicated period of time with BYL719 (5μM), were analyzed by immunoblotting with the indicated antisera.
(F) BPC or B10C melanoma cells were cultured in the presence of BYL719 (5μM), LGX818 (100nM) or the combination of both agents with cells fixed and stained with Crystal Violet every 24 hours for a total period of 72 hours. Crystal Violet staining was quantified as described above. Error bars represent SEM. Asterisks indicate significant difference between combination drug treatment and LGX818 treatment (multiple *t*-tests, *p<0.05*).
(G) Lysates of BPC or B10C melanoma cells treated for 6 hours with DMSO, LGX818 (100nM), BYL719 (5μM) or the combination of both agents were analyzed by immunoblotting.
(H) BRAF^{V600E}/PIK3CA^{H1047R} melanomas were initiated in suitably manipulated adult *Tyr::CreER, BRaf^{CA}; Pik3ca^{lat}* mice. Following randomization, mice were treated with vehicle, BYL719 (50mg/kg, b.i.d.), LGX818 (30mg/kg, q.d.) or the combination of both agents. Melanoma growth or regression was measured weekly with digital calipers over the course of 40 days of continuous drug treatment. Tumor sizes are displayed as the average percent change in tumor size from the start of treatment, with error bars indicating SEM. Asterisks indicate significant difference between combination drug treatment and LGX818 drug treatment (2-way ANOVA, *p<0.0001*).
(I) A waterfall plot of the best tumor response for each of the 29 mice that received vehicle versus drug treatment in **(H)**. The percent change in tumor size from the start of treatment is shown on the *y*-axis. Negative values indicate tumor shrinkage. Asterisks indicate significant difference between combination drug treatment and BYL719 (blue) or LGX818 (pink) (Unpaired *t*-test, *, *p<0.05, ****, p<0.0001*).

significantly more potent melanoma regression than that observed with LGX818 monotherapy (Fig. 1H). Analysis of the best overall response by waterfall plot indicated that only 2/8 mice treated with BYL719 displayed >30% melanoma regression, which qualifies as a partial response (PR) by modified RECIST 1.1 guidelines (Fig. 1I) (46). By contrast, 7/7 mice treated with LGX818 exceeded the 30% regression threshold, as did 8/8 mice receiving BYL719+LGX818. Finally, combined treatment with LGX818 plus BYL719 provided significantly superior melanoma regression compared to single agent LGX818 therapy (Fig. 1I).

Analysis of glioblastoma, breast or prostate cancer models suggests that PI3'-kinase-β (PI3Kβ/PIK3CB) is the predominant driver of PI3'-lipid production in $PTEN^{Null}$ tumors (47, 48). Consequently, we tested the effects of PI3Kβ selective inhibition on the proliferation of human $BRAF^{V600E}/PTEN^{Null}$ melanoma-derived cells. Two structurally distinct PI3Kβ selective inhibitors were used: GSK2636771 (GSK771) and KIN193 (49-51). Perhaps surprisingly, even at the highest concentration tested (10μM), GSK771 failed to reach the GI_{50} of $BRAF^{V600E}/PTEN^{Null}$ human melanoma cells (Fig. 2A and Fig. S2A). Further, even at 5μM, GSK771 elicited only a minor reduction of pAKT in $BRAF^{V600E}/PTEN^{Null}$ melanoma cells, with no effects on the phosphorylation of downstream PI3K pathway components (Fig. 2B and Fig. S2B). While KIN193 displayed enhanced—but still modest—anti-proliferative activity compared to GSK771, the anti-proliferative activity of KIN193 on PI3Kα-dependent BPC cells (Fig. S2A) suggests that at higher concentrations, the anti-proliferative activity of KIN193 is likely due to inhibition of PI3Kα. Additionally, although 5μM KIN193 modestly suppressed pAKT in some human-derived $BRAF^{V600E}/PTEN^{Null}$ melanoma cells (Fig. 2B and S2B), the ability of 5μM KIN193 treatment to robustly suppress pAKT in PI3Ka-dependent BPC cells (Fig. S2B) further underscores the fact that this activity is likely due to inhibition of PI3Kα.

B10C melanoma cells also displayed proliferative and biochemical resistance to PI3Kβ inhibition (Figs. S2A & S2B). Interestingly, while both KIN193 and GSK771 treatment suppressed pAKT activation in M249 $BRAF^{V600E}/PTEN^{Null}$ melanoma cells, this inhibition did not result in reduced phosphorylation of PRAS40 (Fig. S2B). Moreover, PI3Kβ inhibition had only modest anti-proliferative effects on M249 cells, suggesting that residual PI3Kβ-independent PI3K signaling was sufficient to sustain cell proliferation.

The lack of robust single agent activity on $BRAF^{V600E}/PTEN^{Null}$ melanoma cells observed with PI3Kβ selective inhibition led us to hypothesize that $BRAF^{V600E}/PTEN^{Null}$ human melanoma cells might require the combined activity of PI3Ka and PI3Kb for sustained proliferation. To test this, we assessed cell proliferation of $BRAF^{V600E}/PTEN^{Null}$ cells treated with BYL719 in the presence or absence of a fixed concentration of GSK771 (Fig. 2C). Although PI3Kα inhibition had a modest inhibitory effect on melanoma cell proliferation, the addition of a PI3Kβ inhibitor did not dramatically enhance that effect, suggesting that $BRAF^{V600E}/PTEN^{Null}$ melanoma cells do not rely exclusively on the combined activity of PI3Kα and PI3Kβ for their proliferation.

To test if $BRAF^{V600E}/PTEN^{Null}$ melanoma cells require PI3Kβ to promote PI3'-lipid signaling with downstream effects on cell proliferation we employed GDC-0032, a PI3Kβ-sparing class I PI3K inhibitor that inhibits PI3Kα, δ and γ (52). Initially, we compared the anti-proliferative activity of GDC-0032 to that of GDC-0941, a pan-class I PI3K inhibitor (53). Both GDC-0032 and GDC-0941 displayed equivalent GI_{50} values in all $BRAF^{V600E}/PTEN^{Null}$ melanoma cells tested (Figs. 2D & S2C). Further, treatment with GDC-0032 elicited a dose-dependent reduction in pAKT and its downstream effectors with modestly enhanced potency compared to GDC-0941 (Figs. 2E & S2D). Taken together, these data indicate that

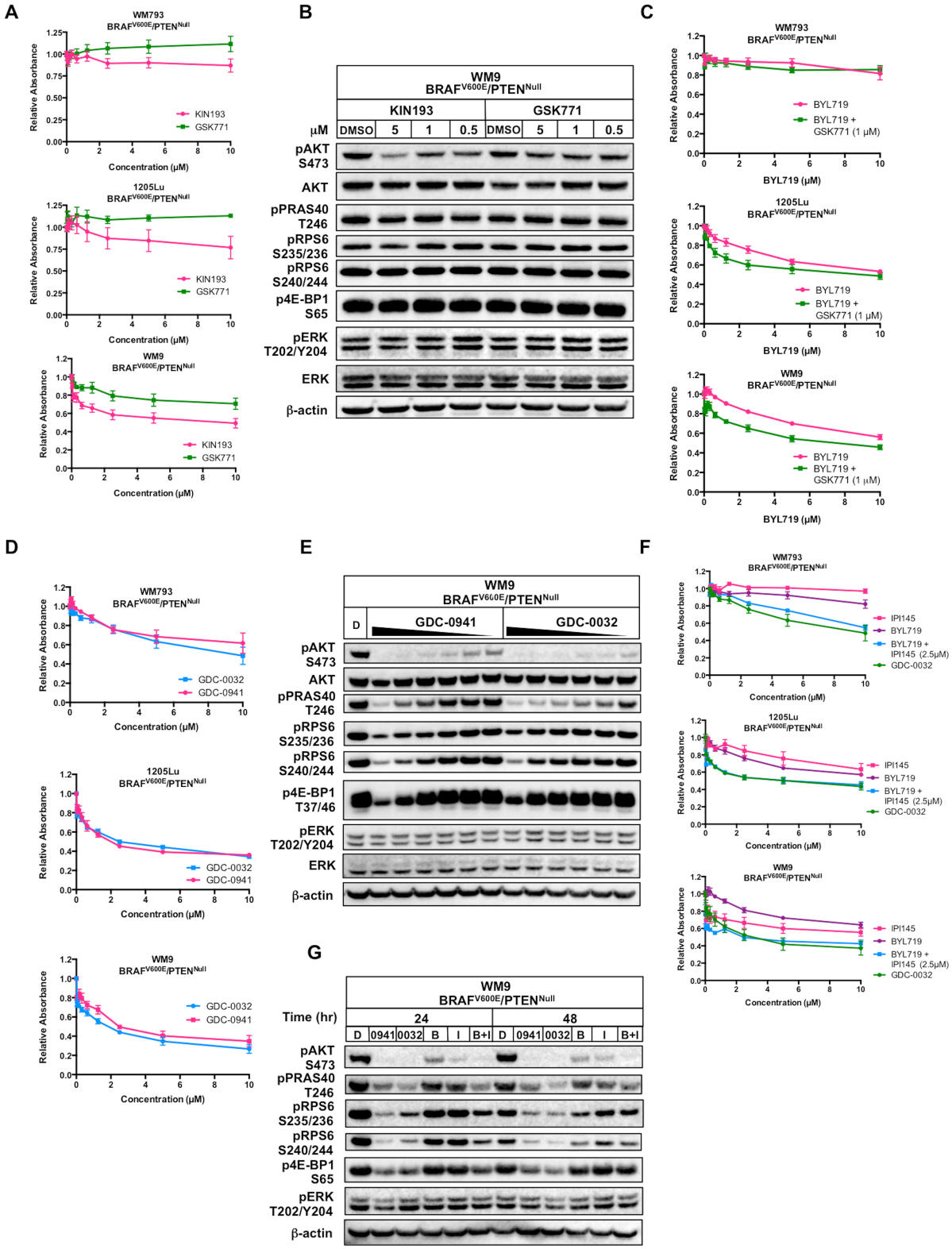

Figure 2: BRAF^{V600E}/PTEN^{Null} human melanoma-derived cells are insensitive to PI3Kβ-selective inhibition but sensitive to PI3Kβ-sparing class I PI3K inhibition

Figure 2 cont.: $BRAF^{V600E}/PTEN^{Null}$ human melanoma-derived cells are insensitive to PI3Kβ-selective inhibition but sensitive to PI3Kβ-sparing class I PI3K inhibition

(A) WM793, 1205Lu or WM9 melanoma cells were cultured in the presence of the indicated concentrations of KIN193 or GSK771 for 72 hours before being fixed and stained with Crystal Violet. Crystal Violet staining was quantified as described above. Values indicated are normalized to DMSO control and error bars represent SEM.
(B) Lysates of WM9 melanoma cells treated for 24 hours with the indicated concentrations of KIN193 or GSK771 were analyzed by immunoblotting.
(C) WM793, 1205Lu or WM9 melanoma cells were cultured in the presence of the indicated concentrations of BYL719 (pink) or BYL719 plus GSK771 (1μM, green) for 72 hours prior to fixation and staining with Crystal Violet. Crystal Violet staining was quantified as described above. Values indicated are normalized to DMSO control and error bars represent SEM.
(D) WM793, 1205Lu or WM9 melanoma cells were cultured in the presence of the indicated concentrations of GDC-0032 (blue) or GDC-0941 (pink) for 72 hours prior to fixation and staining with Crystal Violet. Crystal Violet staining was quantified as described above. Values indicated are normalized to DMSO control and error bars represent SEM.
(E) Lysates of WM9 melanoma cells, treated for 24 hours with DMSO, GDC-0941 or GDC-0032, with drug treatment applied in a serial two-fold dilution series from 10μM to 31.25 nM as indicated by gradient, were analyzed by immunoblotting.
(F) WM793, 1205Lu or WM9 melanoma cells were cultured in the presence of the indicated concentrations of IPI145 (pink), BYL719 (purple), BYL719 + 2.5μM IPI145 (blue) or GDC-0032 (green) for 72 hours prior to fixation and staining with Crystal Violet. Crystal Violet staining was quantified as described above. Values indicated are normalized to DMSO control and error bars represent SEM.
(G) Lysates of WM9 melanoma cells treated for the indicated time period with DMSO **(D)**, GDC-0941 (0941), GDC-0032 (0032), BYL719 (B), IPI145 (I) or BYL719+IPI145 (B+I) (all at 5μM) were analyzed by immunoblotting.

PI3Kb contributes little or nothing to PI3'-lipid signaling or proliferation of $BRAF^{V600E}/PTEN^{Null}$ melanoma cells.

To confirm that $BRAF^{V600E}/PTEN^{Null}$ melanoma cells rely on the combined activity of PI3Kα plus PI3Kδ and/or PI3Kγ for sustained proliferation, we investigated whether the effects of GDC-0032 could be mimicked by combined use of PI3Kα (BYL719) and PI3Kδ/γ (IPI145) selective inhibitors (54). Treatment of $BRAF^{V600E}/PTEN^{Null}$ WM793, 1205Lu or WM9 human melanoma cells with single agent BYL719 or IPI145 failed to reach the GI_{50}, even at 10μM (Fig. 2F). However, when the cells were treated with a fixed concentration of IPI145 (2.5μM) in the presence of BYL719, the combination elicited a more robust anti-proliferative response similar to the effects of GDC-0032 (Fig. 2F). Furthermore, while single agent treatment of WM9 cells with either BYL719 or IPI145 elicited only a modest reduction in pAKT with little or no effect on downstream pathway components, the combination of BYL719 plus IPI145 elicited a complete and sustained inhibition of pAKT that mirrored the effects of GDC-0032 (Fig. 2G). Similar results were obtained with 1205Lu $BRAF^{V600E}/PTEN^{Null}$ melanoma cells (Fig. S2E). Together, these results suggest that PI3Kβ activity is dispensable for the proliferation and PI3K pathway activation of $BRAF^{V600E}/PTEN^{Null}$ melanoma cells and that these cells instead rely upon the combined activities of PI3Kα, δ and/or γ.

To determine if a PI3Kβ-sparing PI3K inhibitor might augment the effects of $BRAF^{V600E}$ pathway-targeted inhibition, we treated $BRAF^{V600E}/PTEN^{Null}$ human or mouse melanoma cells with GDC-0973 (an inhibitor of MEK1/2), GDC-0032, or GDC-0973 plus GDC-0032 (Figs. 3A & S3A) (55). Importantly, the combined use of these agents elicited robust suppression of pAKT and pERK, as well as more robust suppression of pRPS6 and p4EB-P1 than that achieved with either single agent alone. Additionally, whereas single agent GDC-0973 or GDC-0032

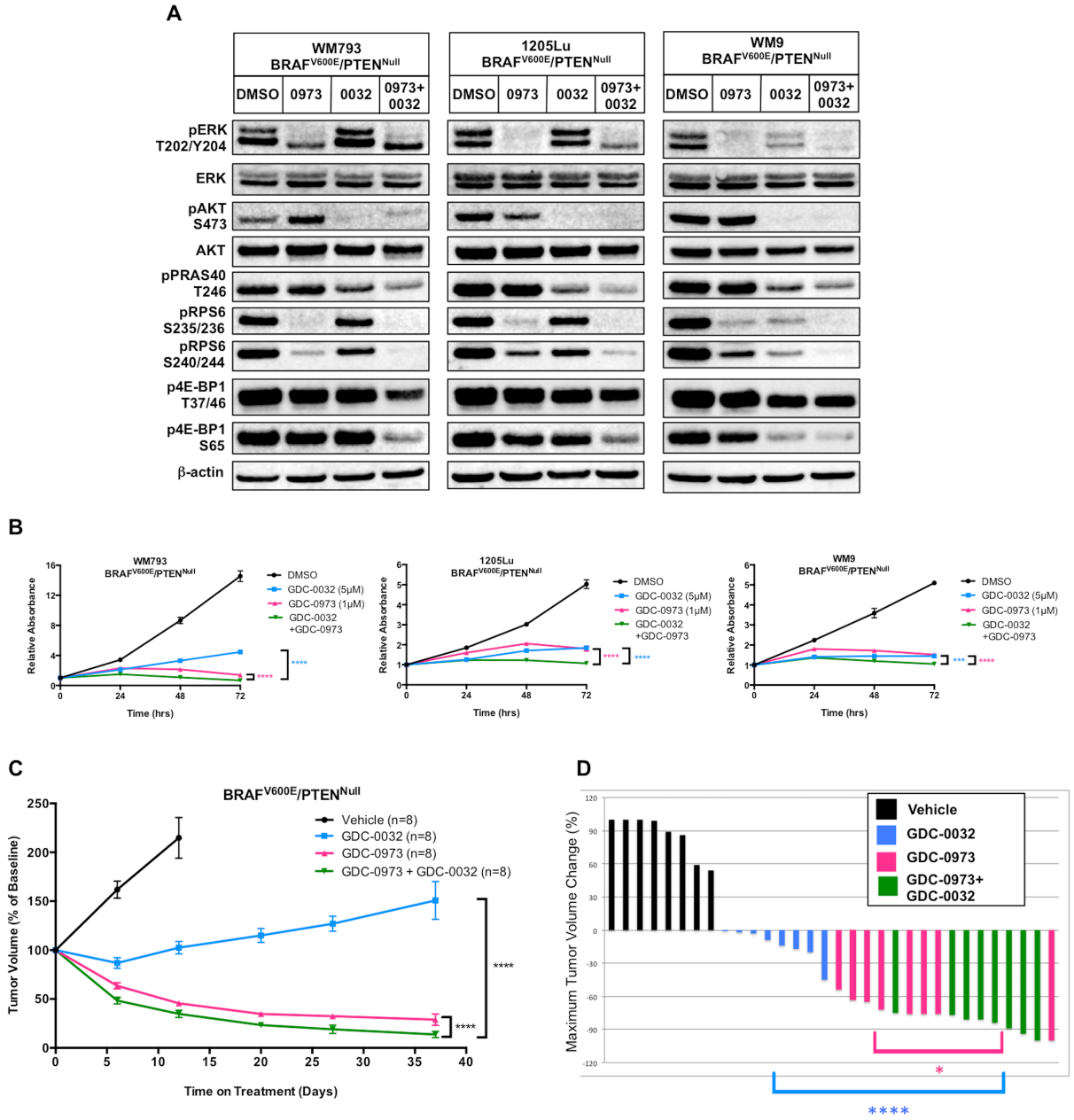

Figure 3: A PI3Kb-sparing inhibitor enhances the effects of MEK1/2 inhibition on both BRAF^{V600E}/PTEN^{Null} human melanoma cells and autochthonous mouse melanomas.

(A) Lysates of WM793, 1205Lu or WM9 melanoma cells treated for 6 hours with GDC-0973 (1μM, 0973), GDC-0032 (5μM, 0032) or GDC-0973 plus GDC-0032 (0973+0032) were analyzed by immunoblotting.

(B) WM793, 1205Lu or WM9 melanoma cells were cultured in the presence of GDC-0032 (5μM), GDC-0973 (1μM) or GDC-0973 plus GDC-0032 with cells fixed and stained with Crystal Violet every 24 hours for of 72 hours. Crystal Violet staining was quantified as described above. Error bars represent SEM. Asterisks indicate significant difference between combination drug treatment and single agent drug treatment (2-way ANOVA, ***, *p<0.0005,*

Figure 3 cont.: A PI3Kb-sparing inhibitor enhances the effects of MEK1/2 inhibition on both BRAF^{V600E}/PTEN^{Null} human melanoma cells and autochthonous mouse melanomas.

(B cont.) ****, *p<0.0001*).

(C) BRAF^{V600E}/PTEN^{Null} melanomas were initiated in suitably manipulated adult *Tyr::CreER, BRaf^{CA}; Pten$^{lox/lox}$* mice. Following randomization, mice were treated with vehicle, single agent or combination GDC-0032 (22.5mg/kg) and GDC-0973 (4.5mg/kg, q.d.). Melanoma growth or regression was measured weekly with digital calipers over the course of 37 days of continuous drug treatment. Mice received GDC-0032 (as single agent or combination therapy) on a b.i.d. regimen for the first 12 days of treatment, but due to apparent toxicity, mice were dosed daily starting on day 13. Tumor sizes are displayed as the average percent change in tumor size from the start of treatment, with error bars indicating SEM. Asterisks indicate significant difference between combination drug treatment and single agent drug treatment (2-way ANOVA, *p<0.0001*).

(D) A waterfall plot of the best tumor response for each of the 32 mice that received vehicle versus drug treatment in (C). The percent change in tumor size from the start of treatment is shown on the *y*-axis. Negative values indicate tumor shrinkage. Asterisks indicate significant difference between combination drug treatment and GDC-0032 (blue) or GDC-0973 (pink) (Unpaired *t*-test, *, *p<0.05, ****, p<0.0001*).

suppressed $BRAF^{V600E}/PTEN^{Null}$ human or mouse melanoma cell proliferation, combined treatment elicited a significant reduction in proliferation compared to either single agent alone (Figs. 3B & S3B).

The *in vitro* activity of GDC-0032 against $BRAF^{V600E}/PTEN^{Null}$ melanoma cells prompted us to conduct a preclinical trial to test the ability of GDC-0032 to elicit regression of $BRAF^{V600E}/PTEN^{Null}$ melanomas *in vivo*, either alone or in combination with GDC-0973. To that end, $BRAF^{V600E}/PTEN^{Null}$ melanoma was initiated in adult *Tyr::CreER; BRaf^{CA}; Pten$^{lox/lox}$* mice and, seven weeks p.i., mice were randomized to receive vehicle, GDC-0973, GDC-0032 or combination therapy with melanoma size measured weekly (Fig. 3C). As with $BRAF^{V600E}/PIK3CA^{H1047R}$ melanomas treated with BYL719, inhibition of PI3K signaling with GDC-0032 had largely cytostatic effects on $BRAF^{V600E}/PTEN^{Null}$ melanomas (Figs. 3C & 3D). By contrast, MEK1/2 inhibition with GDC-0973 elicited substantial regression of $BRAF^{V600E}/PTEN^{Null}$ melanomas, which was significantly enhanced by combined treatment with GDC-0032 (Figs. 3C & 3D).

To investigate the potential role of PI3Kβ in *BRAF*-mutated melanoma cells in which there is no documented genetic alteration in components of PI3K signaling, we treated SK-MEL-239 human melanoma cells ($BRAF^{V600E}/PTEN^{WT}$) with inhibitors of PI3Kβ, and characterized the anti-proliferative response (Fig. S4A). While we observed modestly enhanced potency for KIN193 as compared to GSK771, the GI_{50} for both PI3Kβ inhibitors on SK-MEL-239 melanoma cells was >10μM. While SK-MEL-239 cells exhibit low basal levels of pAKT, inhibition of PI3Kβ did not suppress activation of downstream pathway components pPRAS40, pRPS6, or p4E-BP1 (Fig. S4B). Moreover, both GDC-0032 and GDC-0941 displayed equivalent GI_{50} values in SK-MEL-239 cells (Fig. S4C). The combined use of GDC-0032 plus GDC-0973

elicited robust suppression of pAKT and pERK, as well as an even more robust suppression of pRPS6 and p4E-BP1 than that achieved with either single agent (Fig. S4D). Finally, whereas single agent GDC-0973 or GDC-0032 suppressed SK-MEL-239 cell proliferation, combined treatment elicited a significant reduction in proliferation compared to either single agent alone (Figs. S4E). Collectively these results indicate that, in at least one $BRAF^{V600E}$/$PTEN^{WT}$ human melanoma cell line, PI3Kβ activity is dispensable for proliferation and that these cells rely upon the combined activities of PI3Kα, δ and/or γ.

Although the majority of *BRAF*-mutated melanoma patients experience initial tumor regression in response to $BRAF^{V600E}$ pathway-targeted therapies, the durability of response is limited by the onset of drug resistant disease (32). Therefore, we wished to test if inhibition of class I PI3K isoform(s) would influence the development of resistance to inhibitors that target $BRAF^{V600E}$ signaling. We initially tested this question using vehicle-treated $BRAF^{V600E/}PTEN^{Null}$ melanoma-bearing mice enrolled in the study described in Fig. 3C. When these mice (n=8) were near to end-stage, they were randomly re-assigned to receive extended treatment with either GDC-0973 monotherapy or combined GDC-0973 plus GDC-0032. These mice received a reduced dose of GDC-0973 (2mg/kg) and a full dose GDC-0032 (22.5mg/kg) to minimize the toxicity of full dose combination therapy. As expected, mice in both treatment groups experienced initial tumor regression, which was superior with combined treatment compared to GDC-0973 monotherapy (Figs. 4A and 4B). However, over the course of 113 days of treatment, all of the mice receiving GDC-0973 monotherapy developed drug resistant disease, defined as tumor re-growth ≥100% of the tumor volume at the initiation of therapy. By contrast, none of the mice receiving combination therapy developed drug resistant disease. To further investigate the role of PI3K pathway activity in promoting resistance to GDC-0973 treatment,

when the first mouse receiving GDC-0973 monotherapy reached end-stage, the tumor was resected, fragmented, and implanted into a cohort (n=8) of immunocompromised mice. Immediately following implantation, these mice received GDC-0973 monotherapy treatment. As expected, the transplanted tumor displayed resistance to GDC-0973 and grew progressively over 50 days. At this time, half of the mice were randomly re-assigned to receive GDC-0973 plus GDC-0032 combination therapy, while the rest continued to receive GDC-0973 monotherapy (Fig. 4C). The mice receiving GDC-0973 plus GDC-0032 combination therapy experienced potent tumor cytostasis, suggesting that PI3K pathway activity is necessary for the sustained growth of a melanoma that has developed resistance to a MEK1/2 inhibitor.

To further validate the ability of PI3K inhibitors to forestall the onset of resistance to targeted blockade of $BRAF^{V600E}$ signaling, $BRAF^{V600E}$/$PIK3CA^{H1047R/H1047R}$ melanoma was initiated in 13 adult *Tyr::CreER; $BRaf^{CA}$; $Pik3ca^{lat/lat}$* mice and, 61 days p.i., mice were randomized to receive GDC-0973 (2mg/kg) monotherapy or GDC-0973 plus BYL719 (50mg/kg) combination therapy. As observed with $BRAF^{V600E}$/$PTEN^{Null}$ driven melanomas, mice in both treatment groups experienced initial tumor regression, which was superior with combined treatment compared to GDC-0973 monotherapy (Figs. 4D and 4E). However, over the course of 106 days, 6/7 mice receiving GDC-0973 monotherapy developed drug resistant disease. By contrast, none of the mice receiving combination therapy developed drug resistance.

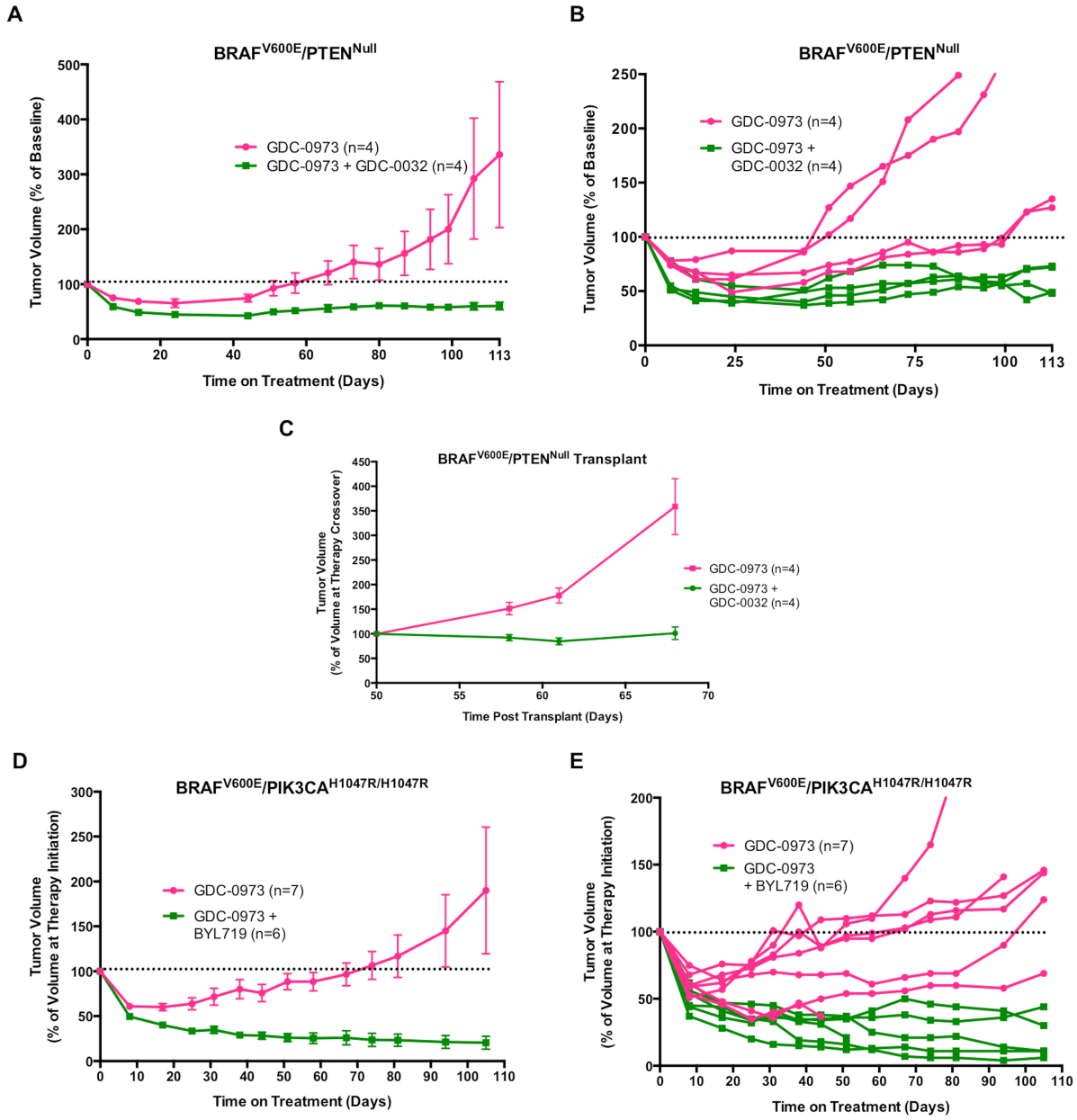

Figure 4: PI3K inhibition forestalls the development of MEK1/2 inhibitor resistance in two different GEM models of melanoma.

(A) After two weeks of vehicle treatment, $BRAF^{V600E}/PTEN^{Null}$ melanoma-bearing mice from the experiment described in Fig. 3C were crossed over to receive either GDC-0973 (2mg/kg) or GDC-0973 (2mg/kg) plus GDC-0032 (22.5mg/kg). Tumors were measured weekly with digital calipers with tumor size displayed as the average percent change in tumor size from the initiation of drug treatment, with error bars indicating SEM.

(B) A spider plot of the individual tumor response for each of the eight mice treated in **(E)**. Horizontal dotted line indicates progressive disease when tumor volume was $\geq$100% of tumor volume prior to drug treatment. Tumor sizes are displayed as the average percent change in tumor size from the crossover point.

Figure 4 cont.: PI3K inhibition forestalls the development of MEK1/2 inhibitor resistance in two different GEM models of melanoma.

(C) Fragments of a single GDC-0973 resistant tumor from (A) were implanted into eight immunocompromised mice and allowed to grow into measurable tumors over 50 days with daily administration of GDC-0973 (2mg/kg). At that time, mice were randomized to receive either combination GDC-0973 (2mg/kg) plus GDC-0032 (22.5mg/kg) (green) or continuation of single agent GDC-0973 (2mg/kg) (pink). Tumor sizes were measured weekly and plotted as described previously. Tumor sizes are displayed as the average percent change in tumor size from the crossover point, with error bars indicating SEM.

(D) $BRAF^{V600E}$/$PIK3CA^{H1047R}$ melanomas were initiated in 13 adult *Tyr::CreER; BRaf*^{CA}*; Pik3ca*$^{lat/lat}$ mice and 8 weeks later they were randomized by tumor size and sex for treatment with GDC-0973 (2mg/kg, q.d., n=7) or GDC-0973 plus BYL719 (50mg/kg, b.i.d., n=6). Melanoma growth or regression was measured weekly over the course of 106 days of drug treatment. Tumor sizes were measured weekly and plotted as described previously, with error bars indicating SEM.

(E) A spider plot of the individual tumor response for each of the 13 mice treated in (D). Horizontal dotted line indicates progressive disease when tumor volume was $\geq$100% of tumor volume prior drug treatment. Tumor sizes are displayed as the average percent change in tumor size from the start of treatment.

Discussion

At the initiation of these studies, the high rate of *PTEN* silencing compared to mutational activation of *PIK3CA* suggested that PTEN might exert PI3'-lipid phosphatase-independent tumor suppressor functions to restrain progression of *BRAF*-mutated melanoma (37). We previously noted that, while heterozygous mutational activation of *Pik3ca*^{lat} was sufficient to promote melanoma progression, BRAF^{V600E}/PIK3CA^{H1047R} melanomas grew significantly more slowly than did BRAF^{V600E}/PTEN^{Null} melanomas (35). However, BRAF^{V600E}-driven melanomas homozygous for PIK3CA^{H1047R} expression grew even more rapidly than BRAF^{V600E}/PTEN^{Null} melanomas. Although we cannot formally exclude a role for PI3'-lipid phosphatase-independent PTEN tumor suppressor functions to restrain progression of *BRAF*-mutated melanoma, there is no compelling rationale to invoke such mechanisms. Importantly, the correlation between PI3K pathway activation and melanoma growth rate indicates that PI3K catalytic isoforms are relevant drug targets in the treatment of BRAF^{V600E}/PTEN^{Null} melanoma.

The "oncogene addiction" hypothesis posits that, despite a high burden of genetic damage, tumors remain dependent on the sustained activity of one or a small number of oncogenes for maintenance of the malignant phenotype (56). As a corollary, inhibition of the oncogene(s) to which a tumor is addicted can elicit profound tumor regression (57). Accordingly, our model of BRAF^{V600E}/PIK3CA^{H1047R} melanoma is driven by two oncogene activation events one of which, BRAF^{V600E}, drives tumor initiation and the other of which, PIK3CA^{H1047R}, promotes melanoma progression (45). Potent inhibitors of either BRAF^{V600E} or PIK3CA^{H1047R} allowed us to characterize to which of these two oncoproteins are BRAF^{V600E}/PIK3CA^{H1047R} melanomas most addicted *in vivo*. While inhibition of BRAF^{V600E} elicited profound melanoma regression, selective inhibition of PIK3CA^{H1047R} elicited largely

cytostatic effects: only 2/8 mice displayed a ≥30% reduction in melanoma size in response to BYL719 monotherapy and that response was largely transient (46). These results may illustrate a fundamental difference between the effects of oncogenic $BRAF^{V600E}$ and $PIK3CA^{H1047R}$ on the sustained survival of melanoma cells, carrying potential clinical implications.

Previous studies of PTEN deficient tumor cells have indicated that PI3Kβ is an essential contributor to PI3'-lipid signaling and aberrant cell proliferation (47, 48). However, our work suggests that PI3Kβ, either alone or in combination with PI3Ka, does not contribute to PI3'-lipid signaling or to the proliferation of human or mouse $BRAF^{V600E}$/$PTEN^{Null}$ melanoma cells. Although PI3Kβ inhibitors modestly attenuated pAKT in M249 cells, this did not translate into suppression of cell proliferation. Furthermore, a PI3Kβ-sparing inhibitor and a combination of agents that inhibits PI3Kα, δ and γ had potent inhibitory effects on PI3'-lipid signaling and proliferation of $BRAF^{V600E}$/$PTEN^{Null}$ melanoma cells. Interestingly, SK-MEL-239 melanoma cells, which express $BRAF^{V600E}$ and normal PTEN, also displayed resistance to PI3Kβ inhibition and equivalent sensitivity to pan class I (GDC-0941) or PI3Kβ-sparing PI3K inhibition (GDC-0032), demonstrating no role for PI3Kβ in these cells. It is tempting to speculate that PI3Kβ may play a role in the proliferation of melanomas in which *RAC1* is mutated or amplified, as PI3Kβ is a direct target of activated RAC1-GTP (27, 58).

Despite the potent biochemical and anti-proliferative effects of the PI3Kβ–sparing inhibitor GDC-0032 *in vitro*, this agent elicited largely cytostatic effects in our $BRAF^{V600E}$/$PTEN^{Null}$ GEM melanoma model and showed modest, but significant, cooperation with MEK1/2 inhibition to promote melanoma regression. Perplexingly, although both human and mouse cancer genetics indicate an important role for PI3K signaling in disease progression, the limited activity of PI3K inhibitors in solid tumor clinical trials does not correlate with PI3K

pathway activation (59). This may be due to a role for PI3K signaling predominantly in promoting cell cycle progression and not for suppression of apoptosis. However, more promisingly, treatment with GDC-0032 forestalled the onset of resistance to a MEK1/2 inhibitor (GDC-0973) in our GEM model of $BRAF^{V600E}$/$PTEN^{Null}$ melanoma. Importantly, upon serial transplantation, MEK1/2 inhibitor resistant melanomas retained sensitivity to combined GDC-0973 plus GDC-0032 treatment, highlighting the importance of PI3K pathway signaling in maintenance of the MEK1/2 inhibitor-resistant phenotype. Further emphasizing the importance of PI3K signaling in MEK1/2 inhibitor resistance, the emergence of GDC-0973 resistant melanomas was forestalled by combined treatment with BYL719 in our $BRAF^{V600E}$/$PIK3CA^{H1047R}$ GEM melanoma model. Since a major limitation in single agent treatment of *BRAF*-mutated melanoma is the onset of drug resistant disease, the observation that PI3K inhibition enhances the depth and durability of response to $BRAF^{V600E}$ pathway-targeted inhibition may illuminate an arena in which PI3K inhibitors will offer substantial clinical benefit.

Materials and Methods

Cell Culture and Drug Treatments

Human melanoma cell lines WM793, WM9, and 1205Lu were kindly provided from the well-curated cell line repository established by Dr. Meenhard Herlyn (Wistar Institute, Philadelphia, PA), and genomic sequencing of these cells was performed in the laboratory of Dr. Katherine Nathanson (University of Pennsylvania, Philadelphia, PA). Human melanoma cell lines M249 and M233 were kindly provided by Dr. Antoni Ribas (University of California, Los Angeles, Los Angeles, CA) and authenticated by genomic sequencing as previously described (60). Human melanoma cell line SK-MEL-239 was kindly provided by Dr. David B. Solit (Memorial Sloan-Kettering Cancer Center, New York, NY) authenticated by genomic sequencing as previously described (18). Mouse melanoma cell lines B10C, BPC, and BP_2C were established as described previously and authenticated by PCR and immunoblot analyses (35). Efficient generation of melanoma cell lines from our various GEM models requires the silencing of the *Cdkn2a* locus encoding INK4A and ARF. Mouse or human melanoma cell lines were cultured as described previously (35). Pathway-targeted pharmacological agents were obtained from various colleagues in the public or private sector or from commercial sources (see Supplementary Table 1 for provenance).

Proliferation and Growth Assays

Melanoma cell proliferation was assessed over 72-hours by seeding 5×10^4 cells in 12-well dishes. Cells were treated with the various pharmacological agents as described with viable

cells enumerated using a Countess® cell counter (Invitrogen). In addition, melanoma cells were seeded and treated with pharmacological agents as described for 72 hours at which time viable cells were stained with crystal violet and quantified by solubilization in 33% acetic acid with A562 absorbance assessed. GI_{50} assays were performed by seeding 8.0 x 10^3 cells in a 96-well plate and treating cells with pharmacological agents as described for 72 hours at which time viable cells were stained with Crystal Violet and quantified by solubilization in 33%(v/v) acetic acid with A562 absorbance assessed. At least three independent experiments, performed in biological triplicate, were completed for all 72-hour assays. Long-term colony formation assays were performed by culturing 500-2000 cells in a 10cm dish for 6-11 days in the absence or presence of various agents with cell colonies fixed and stained with Crystal Violet.

Immunoblot Analysis

Cell lysates were generated for analysis of 50μg aliquots by immunoblotting as described previously (43). Membranes were stained with primary antibodies with antigen-antibody complexes detected using fluorescent goat anti-Rabbit IRDye 800 or goat anti-Mouse IRDye 680 secondary antibodies (LI-COR Biosciences) and visualized with a LI-COR infrared imaging system (Odyssey Fc). Immunoblot data were analyzed using Image Studio v2.0 software (LI-COR Biosciences).

Experimental Animals

The UCSF Institutional Animal Care and Use Committee (IACUC) reviewed and

approved all animal procedures. *Tyr::CreER*, *BRaf*^{CA}, *Pten*$^{lox4-5}$ or *Pik3ca*$^{Lat-1047R}$ mice, maintained on an outbred background, were intercrossed to generate experimental mice which were genotyped as previously described (26, 35). Melanocyte-specific Cre activity was induced in adult mice by topical application of 1.5ml of 5μM 4-hydroxytamoxifen (4-HT, 70% Z-isomer, in 100% Ethanol, Sigma Aldrich) to shaved back skin. Animals were euthanized based on a body conditioning score (61) or when tumor volume $\geq$2cm^3, whichever occurred first. At necropsy, tissue was snap frozen in liquid nitrogen. Tissue was homogenized in RIPA buffer using the Tissue Lyser II (Qiagen®) for immunoblotting as described previously (35).

Treatment of Mice with Pathway-Targeted Inhibitors

Melanoma-bearing mice were divided among treatment arms to give equal distribution of tumor volume and gender when the mean tumor volume of the cohort exceeded 500mm^3. Mice were assigned to receive LGX818 (30mg/kg q.d.) or BYL719 (50mg/kg b.i.d.) formulated in 0.5%(w/v) carboxymethylcellulose/0.5%(v/v) Tween-80 (Sigma Aldrich) or GDC-0973 (2.0 or 4.5mg/kg q.d.) or GDC-0032 (22.5mg/kg q.d.) formulated in 0.5%(w/v) methylcellulose/0.2%(v/v) Tween-80 (Sigma Aldrich) and administered via oral gavage six days per week. Melanoma growth was measured weekly using digital calipers with relative tumor volume (RTV) estimated using the ellipsoid volume formula as described previously (35).

Statistical Analysis

All quantitative data is represented as means ± SEM. GraphPad Prism 6 statistical software was used to determine *p* values for the proliferation graphs by performing two-way ANOVA analysis and *t*-tests as indicated.

References

1. Haass NK, Herlyn M. Normal human melanocyte homeostasis as a paradigm for understanding melanoma. The journal of investigative dermatology Symposium proceedings / the Society for Investigative Dermatology, Inc [and] European Society for Dermatological Research. 2005;10:153-63.
2. Clark WH, Jr., Elder DE, Guerry Dt, Epstein MN, Greene MH, Van Horn M. A study of tumor progression: the precursor lesions of superficial spreading and nodular melanoma. Human pathology. 1984;15:1147-65.
3. Tsai J, Lee JT, Wang W, Zhang J, Cho H, Mamo S, et al. Discovery of a selective inhibitor of oncogenic B-Raf kinase with potent antimelanoma activity. Proceedings of the National Academy of Sciences of the United States of America. 2008;105:3041-6.
4. Flaherty KT, Puzanov I, Kim KB, Ribas A, McArthur GA, Sosman JA, et al. Inhibition of mutated, activated BRAF in metastatic melanoma. The New England journal of medicine. 2010;363:809-19.
5. Sosman JA, Kim KB, Schuchter L, Gonzalez R, Pavlick AC, Weber JS, et al. Survival in BRAF V600-mutant advanced melanoma treated with vemurafenib. The New England journal of medicine. 2012;366:707-14.
6. Chapman PB, Hauschild A, Robert C, Haanen JB, Ascierto P, Larkin J, et al. Improved survival with vemurafenib in melanoma with BRAF V600E mutation. The New England journal of medicine. 2011;364:2507-16.
7. Azam M, Seeliger MA, Gray NS, Kuriyan J, Daley GQ. Activation of tyrosine kinases by mutation of the gatekeeper threonine. Nature structural & molecular biology. 2008;15:1109-18.
8. Whittaker S, Kirk R, Hayward R, Zambon A, Viros A, Cantarino N, et al. Gatekeeper mutations mediate resistance to BRAF-targeted therapies. Sci Transl Med. 2010;2:35ra41.
9. Nazarian R, Shi H, Wang Q, Kong X, Koya RC, Lee H, et al. Melanomas acquire resistance to B-RAF(V600E) inhibition by RTK or N-RAS upregulation. Nature. 2010;468:973-7.
10. Emery CM, Vijayendran KG, Zipser MC, Sawyer AM, Niu L, Kim JJ, et al. MEK1 mutations confer resistance to MEK and B-RAF inhibition. Proceedings of the National Academy of Sciences of the United States of America. 2009;106:20411-6.
11. Van Allen EM, Wagle N, Sucker A, Treacy DJ, Johannessen CM, Goetz EM, et al. The genetic landscape of clinical resistance to RAF inhibition in metastatic melanoma. Cancer discovery. 2014;4:94-109.
12. Clara Montagut SVS, Toshi Shioda, Ultan McDermott, Matthew Ulman, Lindsey E. Ulkus, Dora Dias-Santagata, Hannah Stubbs, Diana Y. Lee, Anurag Singh, Lisa Drew, Daniel A. Haber, and Jeffrey Settleman. Elevated CRAF as a Potential Mechanism of Acquired Resistance to BRAF Inhibition in Melanoma. Cancer Research. 2008;68:4853-61.
13. Su F, Bradley WD, Wang Q, Yang H, Xu L, Higgins B, et al. Resistance to selective BRAF inhibition can be mediated by modest upstream pathway activation. Cancer Res. 2012;72:969-78.
14. Karreth FA, DeNicola GM, Winter SP, Tuveson DA. C-Raf inhibits MAPK activation and transformation by B-Raf(V600E). Mol Cell. 2009;36:477-86.

15. Johannessen CM, Boehm JS, Kim SY, Thomas SR, Wardwell L, Johnson LA, et al. COT drives resistance to RAF inhibition through MAP kinase pathway reactivation. Nature. 2010;468:968-72.
16. Schimke RT, Alt FW, Kellems RE, Kaufman RJ, Bertino JR. Amplification of dihydrofolate reductase genes in methotrexate-resistant cultured mouse cells. Cold Spring Harbor symposia on quantitative biology. 1978;42 Pt 2:649-57.
17. Shi H, Moriceau G, Kong X, Lee MK, Lee H, Koya RC, et al. Melanoma whole-exome sequencing identifies (V600E)B-RAF amplification-mediated acquired B-RAF inhibitor resistance. Nat Commun. 2012;3:724.
18. Poulikakos PI, Persaud Y, Janakiraman M, Kong X, Ng C, Moriceau G, et al. RAF inhibitor resistance is mediated by dimerization of aberrantly spliced BRAF(V600E). Nature. 2011;480:387-90.
19. Kim KB, Kefford R, Pavlick AC, Infante JR, Ribas A, Sosman JA, et al. Phase II study of the MEK1/MEK2 inhibitor Trametinib in patients with metastatic BRAF-mutant cutaneous melanoma previously treated with or without a BRAF inhibitor. Journal of clinical oncology : official journal of the American Society of Clinical Oncology. 2013;31:482-9.
20. Long GV, Stroyakovskiy D, Gogas H, Levchenko E, de Braud F, Larkin J, et al. Combined BRAF and MEK inhibition versus BRAF inhibition alone in melanoma. The New England journal of medicine. 2014;371:1877-88.
21. Larkin J, Ascierto PA, Dreno B, Atkinson V, Liszkay G, Maio M, et al. Combined vemurafenib and cobimetinib in BRAF-mutated melanoma. The New England journal of medicine. 2014;371:1867-76.
22. Shi H, Hugo W, Kong X, Hong A, Koya RC, Moriceau G, et al. Acquired resistance and clonal evolution in melanoma during BRAF inhibitor therapy. Cancer discovery. 2014;4:80-93.
23. Villanueva J, Vultur A, Lee JT, Somasundaram R, Fukunaga-Kalabis M, Cipolla AK, et al. Acquired resistance to BRAF inhibitors mediated by a RAF kinase switch in melanoma can be overcome by cotargeting MEK and IGF-1R/PI3K. Cancer cell. 2010;18:683-95.
24. Dankort D, Filenova E, Collado M, Serrano M, Jones K, McMahon M. A new mouse model to explore the initiation, progression, and therapy of BRAFV600E-induced lung tumors. Genes & development. 2007;21:379-84.
25. Bosenberg M, Muthusamy V, Curley DP, Wang Z, Hobbs C, Nelson B, et al. Characterization of melanocyte-specific inducible Cre recombinase transgenic mice. Genesis. 2006;44:262-7.
26. Dankort D, Curley DP, Cartlidge RA, Nelson B, Karnezis AN, Damsky WE, Jr., et al. Braf(V600E) cooperates with Pten loss to induce metastatic melanoma. Nature genetics. 2009;41:544-52.
27. Hodis E, Watson IR, Kryukov GV, Arold ST, Imielinski M, Theurillat JP, et al. A landscape of driver mutations in melanoma. Cell. 2012;150:251-63.
28. Bastian BC. The molecular pathology of melanoma: an integrated taxonomy of melanocytic neoplasia. Annu Rev Pathol. 2014;9:239-71.
29. Davies H, Bignell GR, Cox C, Stephens P, Edkins S, Clegg S, et al. Mutations of the BRAF gene in human cancer. Nature. 2002;417:949-54.
30. McArthur GC, P.B. Robert, C. et al. Improved survival with vemurafenib in BRAFV600E and BRAFV600K mutation-positive melanoma. Lancet Oncol. 2014;In Press.

31. Hauschild A, Grob JJ, Demidov LV, Jouary T, Gutzmer R, Millward M, et al. Dabrafenib in BRAF-mutated metastatic melanoma: a multicentre, open-label, phase 3 randomised controlled trial. Lancet. 2012;380:358-65.
32. Holderfield M, Deuker MM, McCormick F, McMahon M. Targeting RAF kinases for cancer therapy: BRAF-mutated melanoma and beyond. Nature reviews Cancer. 2014;14:455-67.
33. Lito P, Rosen N, Solit DB. Tumor adaptation and resistance to RAF inhibitors. Nat Med. 2013;19:1401-9.
34. Bucheit AD, Davies MA. Emerging insights into resistance to BRAF inhibitors in melanoma. Biochem Pharmacol. 2014;87:381-9.
35. Marsh Durban V, Deuker MM, Bosenberg MW, Phillips W, McMahon M. Differential AKT dependency displayed by mouse models of BRAFV600E-initiated melanoma. The Journal of clinical investigation. 2013;123:5104-18.
36. Tsao H, Goel V, Wu H, Yang G, Haluska FG. Genetic interaction between NRAS and BRAF mutations and PTEN/MMAC1 inactivation in melanoma. J Invest Dermatol. 2004;122:337-41.
37. Shull AY, Latham-Schwark A, Ramasamy P, Leskoske K, Oroian D, Birtwistle MR, et al. Novel somatic mutations to PI3K pathway genes in metastatic melanoma. PLoS One. 2012;7:e43369.
38. Kim JE, Stones C, Joseph WR, Leung E, Finlay GJ, Shelling AN, et al. Comparison of growth factor signalling pathway utilisation in cultured normal melanocytes and melanoma cell lines. BMC Cancer. 2012;12:141.
39. Shen WH, Balajee AS, Wang J, Wu H, Eng C, Pandolfi PP, et al. Essential role for nuclear PTEN in maintaining chromosomal integrity. Cell. 2007;128:157-70.
40. Song MS, Carracedo A, Salmena L, Song SJ, Egia A, Malumbres M, et al. Nuclear PTEN regulates the APC-CDH1 tumor-suppressive complex in a phosphatase-independent manner. Cell. 2011;144:187-99.
41. Wu H, Goel V, Haluska FG. PTEN signaling pathways in melanoma. Oncogene. 2003;22:3113-22.
42. Furet P, Guagnano V, Fairhurst RA, Imbach-Weese P, Bruce I, Knapp M, et al. Discovery of NVP-BYL719 a potent and selective phosphatidylinositol-3 kinase alpha inhibitor selected for clinical evaluation. Bioorg Med Chem Lett. 2013;23:3741-8.
43. Silva JM, Bulman C, McMahon M. BRAFV600E cooperates with PI3K signaling, independent of AKT, to regulate melanoma cell proliferation. Mol Cancer Res. 2014;12:447-63.
44. Darrin D. Stuart NL, Daniel J. Poon, Kimberly Aardalen, Susan Kaufman, Hanne Merritt, Fernando Salangsang, Edward Lorenzana, Allen Li, Majid Ghoddusi, Giordano Caponigro, Frank Sun, Swarupa Kulkarni, Shefali Kakar, Nancy Turner, Richard Zang, John Tellew, and Nancy Pryer. Preclinical profile of LGX818: A potent and selective RAF kinase inhibitor. Cancer research. 2012;72.
45. Vredeveld LC, Possik PA, Smit MA, Meissl K, Michaloglou C, Horlings HM, et al. Abrogation of BRAFV600E-induced senescence by PI3K pathway activation contributes to melanomagenesis. Genes & development. 2012;26:1055-69.
46. Eisenhauer EA, Therasse P, Bogaerts J, Schwartz LH, Sargent D, Ford R, et al. New response evaluation criteria in solid tumours: revised RECIST guideline (version 1.1). Eur J Cancer. 2009;45:228-47.

47. Wee S, Wiederschain D, Maira SM, Loo A, Miller C, deBeaumont R, et al. PTEN-deficient cancers depend on PIK3CB. Proceedings of the National Academy of Sciences of the United States of America. 2008;105:13057-62.
48. Jia S, Liu Z, Zhang S, Liu P, Zhang L, Lee SH, et al. Essential roles of PI(3)K-p110beta in cell growth, metabolism and tumorigenesis. Nature. 2008;454:776-9.
49. Jackson SP, Schoenwaelder SM, Goncalves I, Nesbitt WS, Yap CL, Wright CE, et al. PI 3-kinase p110beta: a new target for antithrombotic therapy. Nat Med. 2005;11:507-14.
50. Ralph A. Rivero MAH. Identification of GSK2636771, a potent and selective, orally bioavailable inhibitor of phosphatidylinositol 3-kinase-beta (PI3Kα) for the treatment of PTEN deficient tumors. Cancer research. 2012;72.
51. Ni J, Liu Q, Xie S, Carlson C, Von T, Vogel K, et al. Functional characterization of an isoform-selective inhibitor of PI3K-p110beta as a potential anticancer agent. Cancer discovery. 2012;2:425-33.
52. Ndubaku CO, Heffron TP, Staben ST, Baumgardner M, Blaquiere N, Bradley E, et al. Discovery of 2-{3-[2-(1-isopropyl-3-methyl-1H-1,2-4-triazol-5-yl)-5,6-dihydrobenzo[f]imidazo[1 ,2-d][1,4]oxazepin-9-yl]-1H-pyrazol-1-yl}-2-methylpropanamide (GDC-0032): a beta-sparing phosphoinositide 3-kinase inhibitor with high unbound exposure and robust in vivo antitumor activity. J Med Chem. 2013;56:4597-610.
53. Folkes AJ, Ahmadi K, Alderton WK, Alix S, Baker SJ, Box G, et al. The identification of 2-(1H-indazol-4-yl)-6-(4-methanesulfonyl-piperazin-1-ylmethyl)-4-morpholin-4-yl-t hieno[3,2-d]pyrimidine (GDC-0941) as a potent, selective, orally bioavailable inhibitor of class I PI3 kinase for the treatment of cancer. J Med Chem. 2008;51:5522-32.
54. Winkler DG, Faia KL, DiNitto JP, Ali JA, White KF, Brophy EE, et al. PI3K-delta and PI3K-gamma inhibition by IPI-145 abrogates immune responses and suppresses activity in autoimmune and inflammatory disease models. Chem Biol. 2013;20:1364-74.
55. Rice KD, Aay N, Anand NK, Blazey CM, Bowles OJ, Bussenius J, et al. Novel Carboxamide-Based Allosteric MEK Inhibitors: Discovery and Optimization Efforts toward XL518 (GDC-0973). ACS Med Chem Lett. 2012;3:416-21.
56. Weinstein IB. Cancer. Addiction to oncogenes--the Achilles heal of cancer. Science. 2002;297:63-4.
57. Weinstein IB, Joe A. Oncogene addiction. Cancer research. 2008;68:3077-80; discussion 80.
58. Fritsch R, de Krijger I, Fritsch K, George R, Reason B, Kumar MS, et al. RAS and RHO families of GTPases directly regulate distinct phosphoinositide 3-kinase isoforms. Cell. 2013;153:1050-63.
59. Rodon J, Brana I, Siu LL, De Jonge MJ, Homji N, Mills D, et al. Phase I dose-escalation and -expansion study of buparlisib (BKM120), an oral pan-Class I PI3K inhibitor, in patients with advanced solid tumors. Invest New Drugs. 2014;32:670-81.
60. Sondergaard JN, Nazarian R, Wang Q, Guo D, Hsueh T, Mok S, et al. Differential sensitivity of melanoma cell lines with BRAFV600E mutation to the specific Raf inhibitor PLX4032. Journal of translational medicine. 2010;8:39.
61. Ullman-Cullere MH, Foltz CJ. Body condition scoring: a rapid and accurate method for assessing health status in mice. Lab Anim Sci. 1999;49:319-23.

Appendix 1: Supplementary Tables

Supplemental Table 1

Pathway targeted inhibitors that were used to interrogate the role of class I PI3'-kinase isoforms in $BRAF^{V600E}$-driven melanoma

Compound	International Nonproprietary Name	Target	Provenance
GDC0941	Pictilisib	p110α, p110β, p110δ, p110γ	Genentech
GDC0032	Taselisib	p110α, p110δ, p110γ	Genentech
BYL719	Alpelisib	p110α	Novartis
GSK2636771		p110β	Selleckchem
KIN193 (AZD6482)		p110β	Selleckchem
IPI145 (INK1197)		p110δ, p110γ	Selleckchem
LGX818	Encorafenib	BRAF	Novartis
GDC0973	Cobimetinib	MEK1/2	Genentech

Appendix 2: Supplementary Figures

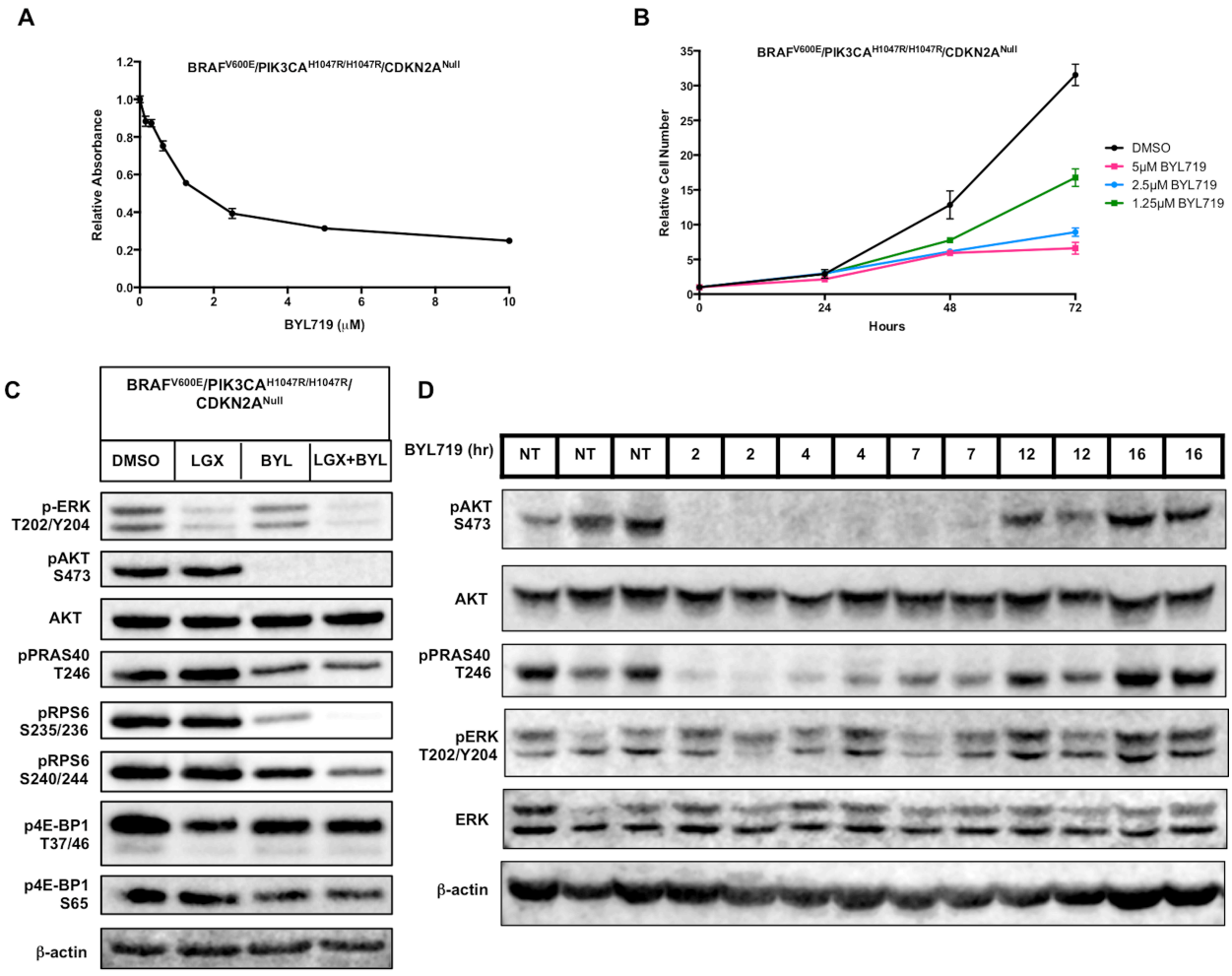

Figure S1: BP_2C mouse melanoma-derived cells are sensitive to PI3Kα-selective inhibition

(A) BP_2C melanoma cells were cultured in the presence of the indicated concentrations of BYL719 for 72 hours before being fixed and stained with Crystal Violet. Crystal Violet staining was quantified as described above. Values are normalized to DMSO control and error bars represent SEM.

(B) BP_2C melanoma cells were cultured in the presence of the indicated concentrations of BYL719 with cells counted every 24 hours for a total period of 72 hours. Cell counts are indicated as change in cell number relative to the number of cells at the initiation of drug treatment and error bars represent SEM.

(C) Lysates of BP_2C melanoma cells treated for 6 hours with DMSO, LGX818 (100nM), BYL719 (5μM) or the combination of both agents were analyzed by immunoblotting.

(D) Mice bearing $BRAF^{V600E}/PIK3CA^{H1047R}$ melanoma were dosed with a single dose of BYL719 (50mg/kg) and sacrificed at the indicated times post dose, with NT indicating no treatment. Lysates of melanomas frozen in liquid nitrogen were analyzed by immunoblotting

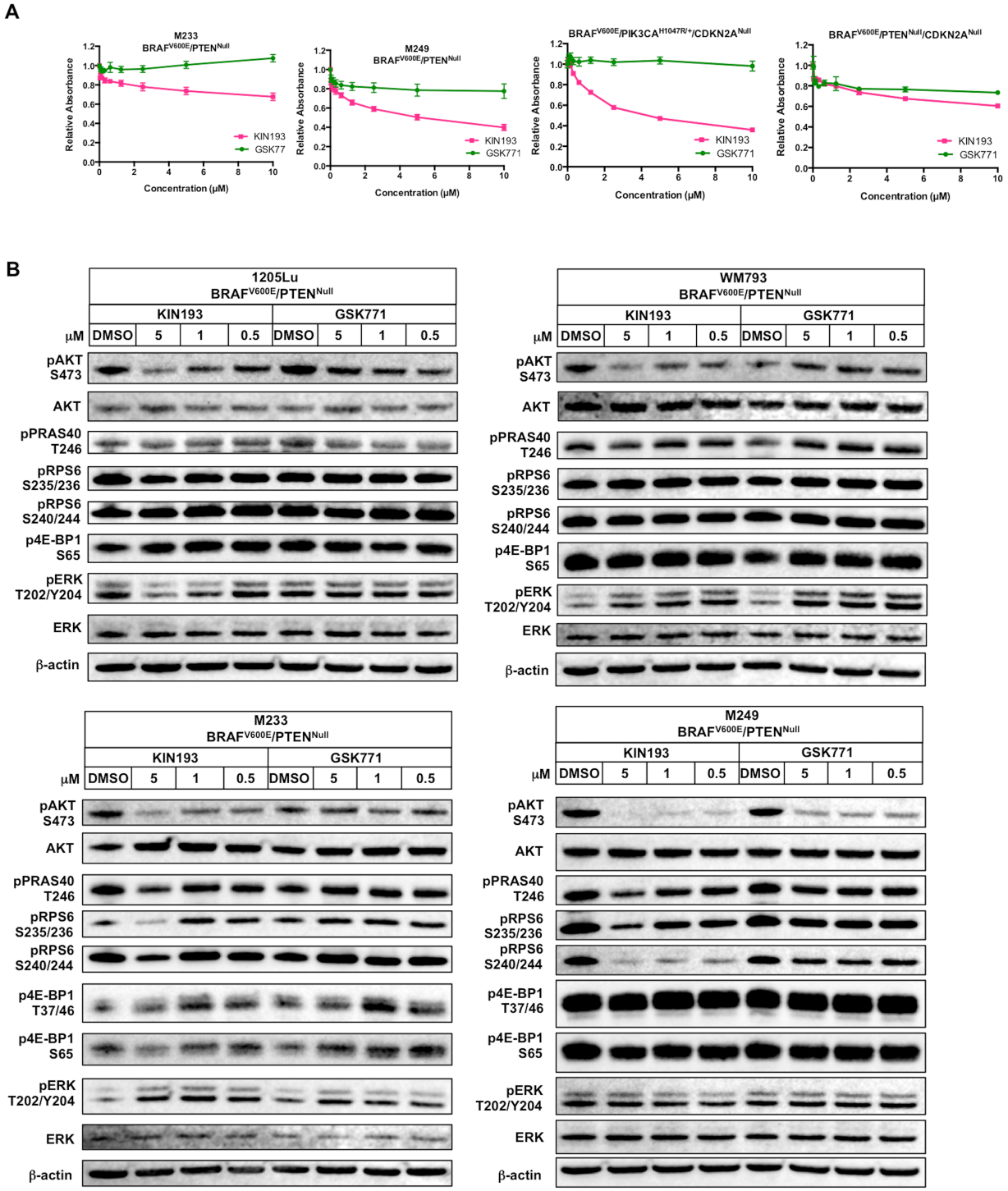

Figure S2: BRAF^{V600E}/PTEN^{Null} melanoma-derived cells are sensitive to PI3Kβ-sparing PI3'-kinase inhibition

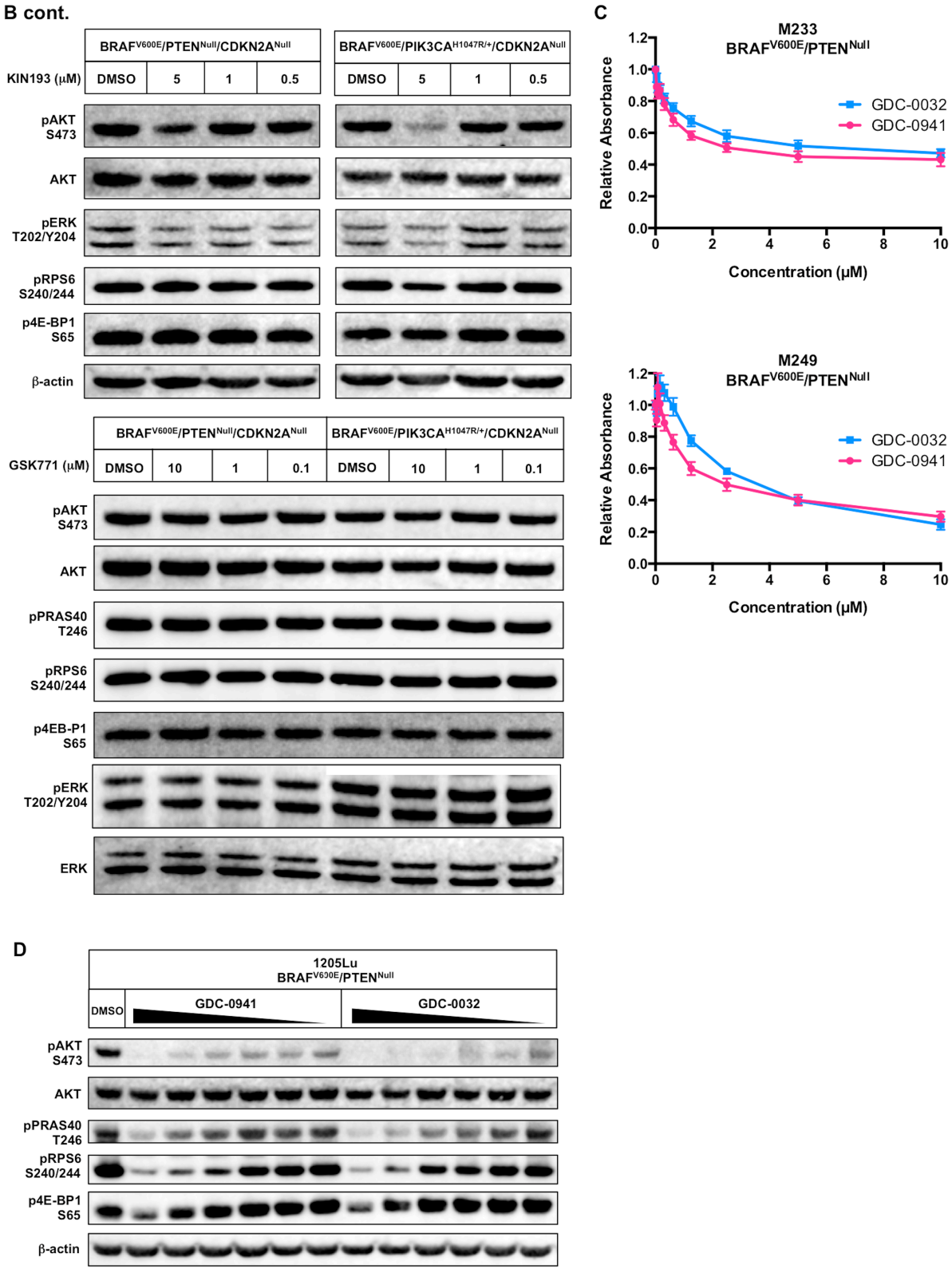

Figure S2 cont.: $BRAF^{V600E}/PTEN^{Null}$ melanoma-derived cells are sensitive to PI3Kβ-sparing PI3'-kinase inhibition

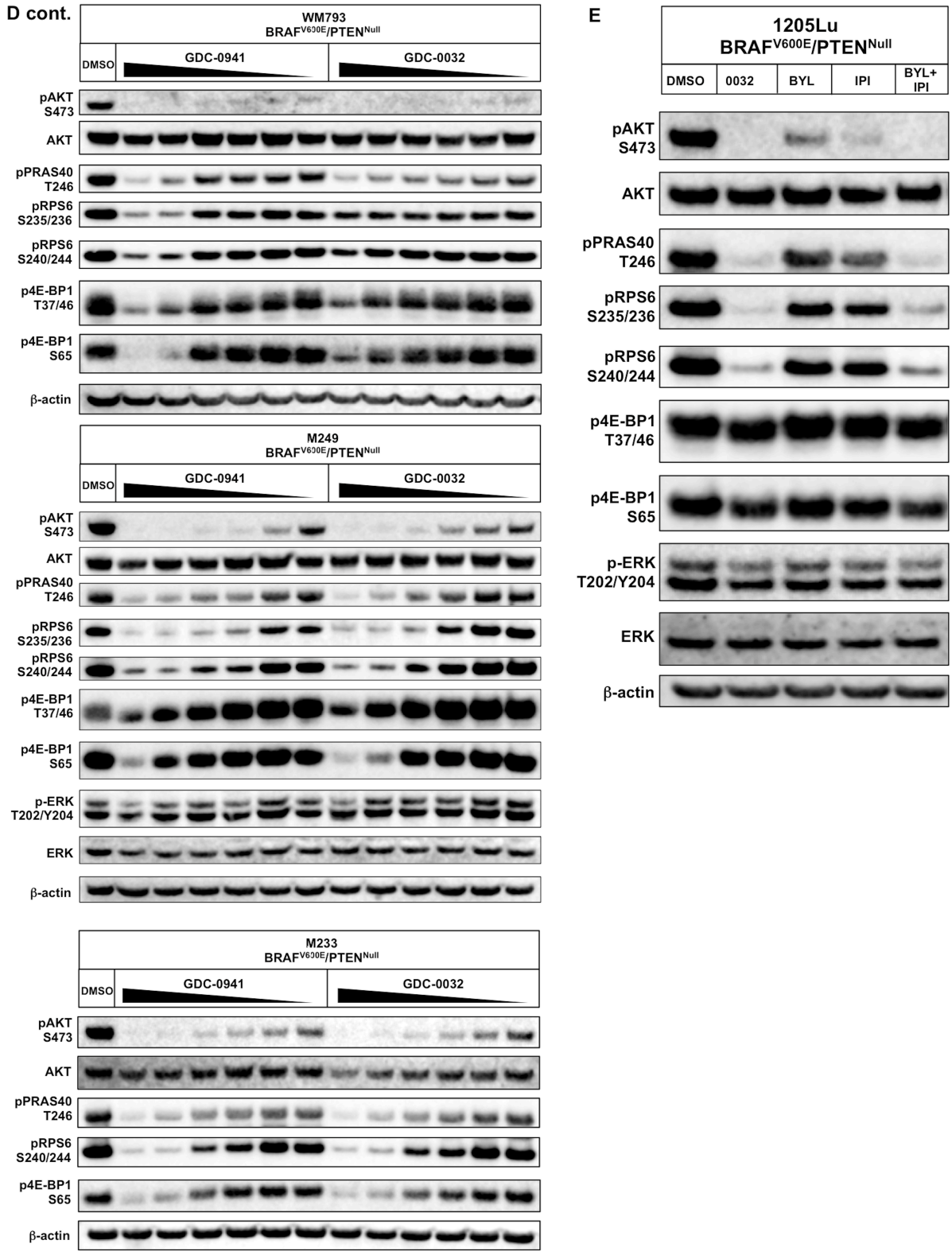

Figure S2 cont.: $BRAF^{V600E}/PTEN^{Null}$ melanoma-derived cells are sensitive to PI3Kβ-sparing PI3'-kinase inhibition

Figure S2 cont.: $BRAF^{V600E}/PTEN^{Null}$ melanoma-derived cells are sensitive to PI3Kβ-sparing PI3'-kinase inhibition

(A) M233 or M249 melanoma cells were cultured in the presence of the indicated concentrations of KIN193 or GSK771 for 72 hours before being fixed and stained with Crystal Violet. Crystal Violet staining was quantified as described above. Values indicated are normalized to DMSO control and error bars represent SEM.
(B) Lysates of 1205Lu, WM793, M233, M249, B10C, or BPC melanoma cells treated for 24 hours with the indicated concentrations of KIN193 or GSK771 were analyzed by immunoblotting.
(C) M233 or M249 melanoma cells were cultured in the presence of the indicated concentrations of GDC-0032 (blue) or GDC-0941 (pink) for 72 hours prior to fixation and staining with Crystal Violet. Crystal Violet staining was quantified as described above. Values indicated are normalized to DMSO control and error bars represent SEM.
(D) Lysates of 1205Lu, WM793, M233 or M249 melanoma cells treated for 24 hours with DMSO or GDC-0941 or GDC-0032 (with drug treatment applied from 10μM to 31.25 nM in two-fold dilution series as indicated) were analyzed by immunoblotting.
(E) Lysates of 1205Lu melanoma cells treated for treated for 24 hours with DMSO, GDC-0032 (0032), BYL719 (BYL), IPI145 (IPI) or BYL719+IPI145 (BYL+IPI) (all at 5μM) were analyzed by immunoblotting.

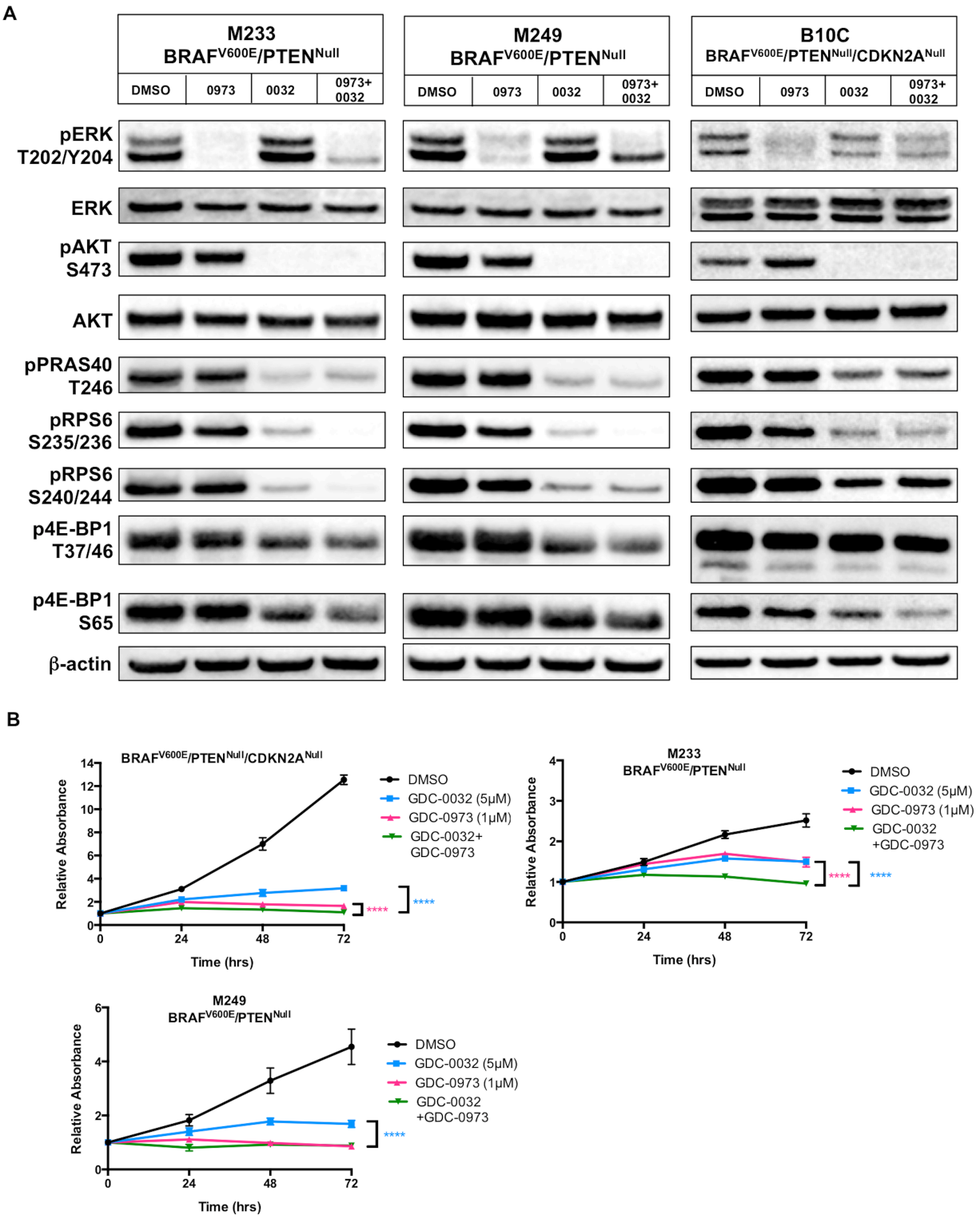

Figure S3: PI3Kβ-sparing PI3K inhibition enhances the effects of MEK inhibition on BRAF^{V600E}/ PTEN^{Null} melanoma-derived cells

A) Lysates of B10C, M233 or M249 melanoma cells treated for 6 hours with GDC-0973 (1μM), GDC-0032 (5μM) or GDC-0973 plus GDC-0032 were analyzed by immunoblotting.

Figure S3: PI3Kβ-sparing PI3K inhibition enhances the effects of MEK inhibition on $BRAF^{V600E}$/ $PTEN^{Null}$ melanoma-derived cells

(B) B10C, M233 or M249 melanoma cells were cultured in the presence of GDC-0032 (5μM), GDC-0973 (1μM) or GDC-0973 plus GDC-0032 with cells fixed and stained with Crystal Violet every 24 hours for of 72 hours. Crystal Violet staining was quantified as described above. Error bars represent SEM. Asterisks indicate significant difference between combination drug treatment and single agent drug treatment (2-way ANOVA, $p<0.0001$).

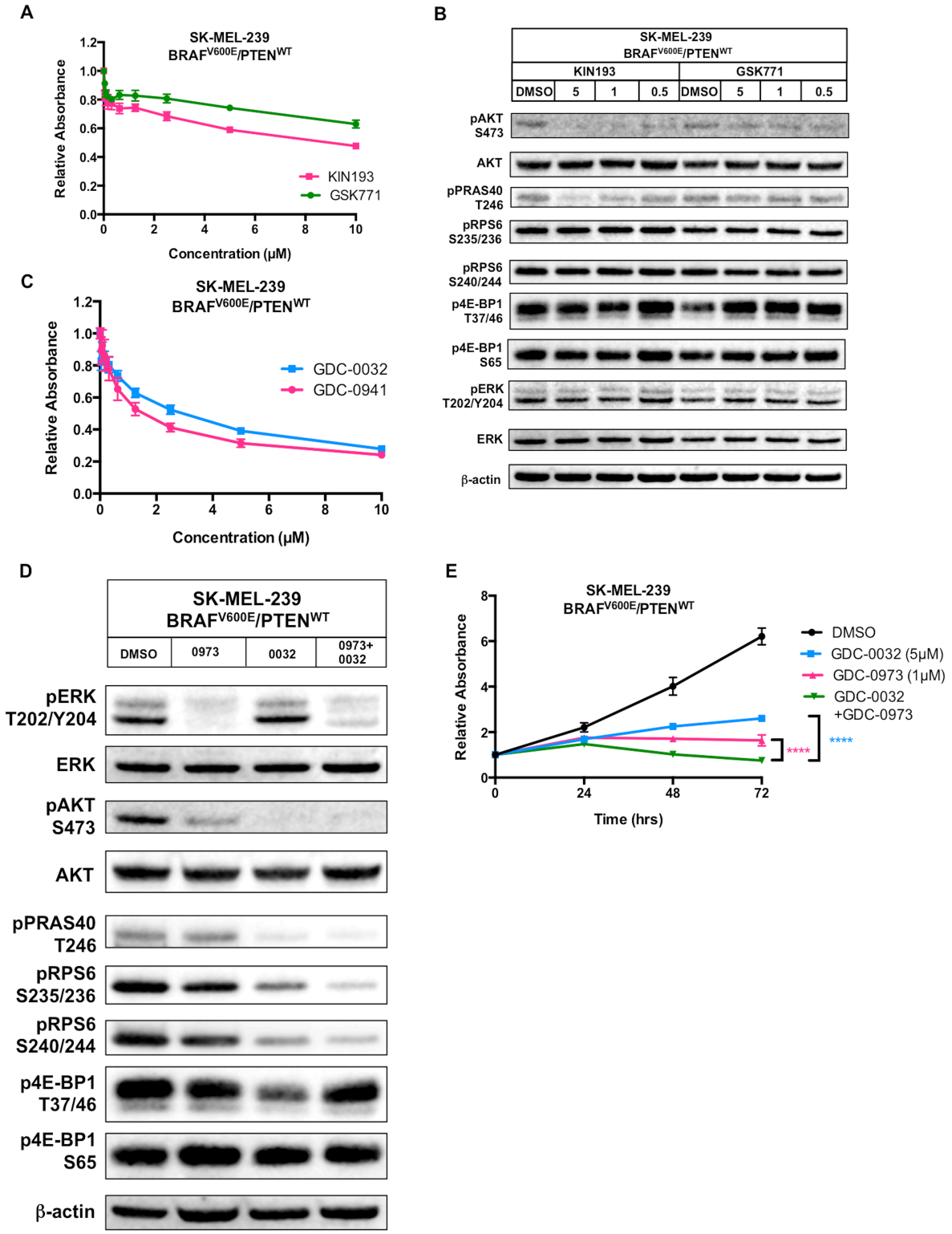

Figure S4: $BRAF^{V600E}/PTEN^{WT}$ melanoma cells are sensitive to PI3Kβ-sparing PI3'-kinase inhibition, and PI3Kβ-sparing PI3K inhibition enhances the effects of MEK inhibition on $BRAF^{V600E}/PTEN^{WT}$ melanoma cells

Figure S4 cont.: $BRAF^{V600E}/PTEN^{WT}$ melanoma cells are sensitive to PI3Kβ-sparing PI3'-kinase inhibition, and PI3Kβ-sparing PI3K inhibition enhances the effects of MEK inhibition on $BRAF^{V600E}/PTEN^{WT}$ melanoma cells

(A) SK-MEL-239 melanoma cells were cultured in the presence of the indicated concentrations of KIN193 or GSK771 for 72 hours before being fixed and stained with Crystal Violet. Crystal Violet staining was quantified as described above. Values indicated are normalized to DMSO control and error bars represent SEM.
(B) Lysates of SK-MEL-239 melanoma cells treated for 24 hours with the indicated concentrations of KIN193 or GSK771 were analyzed by immunoblotting.
(C) SK-MEL-239 melanoma cells were cultured in the presence of the indicated concentrations of GDC-0941 or GDC-0032 for 72 hours before being fixed and stained with Crystal Violet. Crystal Violet staining was quantified as described above. Values indicated are normalized to DMSO control and error bars represent SEM.
(D) Lysates of SK-MEL-239 melanoma cells treated for 6 hours with GDC-0973 (1μM), GDC-0032 (5μM) or GDC-0973 plus GDC-0032 were analyzed by immunoblotting

Publishing Agreement

It is the policy of the University to encourage the distribution of all theses, dissertations, and manuscripts. Copies of all UCSF theses, dissertations, and manuscripts will be routed to the library via the Graduate Division. The library will make all theses, dissertations, and manuscripts accessible to the public and will preserve these to the best of their abilities, in perpetuity.

I hereby grant permission to the Graduate Division of the University of California, San Francisco to release copies of my thesis, dissertation, or manuscript to the Campus Library to provide access and preservation, in whole or in part, in perpetuity.

Author Signature: 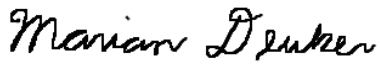 Date: 1 September 2015